SANDIA REPORT

SAND2001-1786
Unlimited Release
Printed June 2001

Lithologic and Structural Controls on Natural Fracture Characteristics Teapot Dome, Wyoming

Scott P. Cooper, John C. Lorenz, and Laurel B. Goodwin

Prepared by
Sandia National Laboratories
Albuquerque, New Mexico 87185 and Livermore, California 94550

Sandia is a multiprogram laboratory operated by Sandia Corporation, a Lockheed Martin Company, for the United States Department of Energy under Contract DE-AC04-94AL85000.

Issued by Sandia National Laboratories, operated for the United States Department of Energy by Sandia Corporation.

Available to DOE and DOE contractors from
U.S. Department of Energy
Office of Scientific and Technical Information
P.O. Box 62
Oak Ridge, TN 37831

Telephone: (865)576-8401
Facsimile: (865)576-5728
E-Mail: reports@adonis.osti.gov
Online ordering: http://www.doe.gov/bridge

Available to the public from
U.S. Department of Commerce
National Technical Information Service
5285 Port Royal Rd
Springfield, VA 22161

Telephone: (800)553-6847
Facsimile: (703)605-6900
E-Mail: orders@ntis.fedworld.gov
Online order: http://www.ntis.gov/ordering.htm

Sand2001-1786
Unlimited Release
Printed June 2001

Lithologic and Structural Controls on Natural Fracture Characteristics Teapot Dome, Wyoming

Scott P. Cooper and John C. Lorenz
Geophysical Technology Department
Sandia National Laboratories
P.O. Box 5800
Albuquerque, NM 87185-0750

Laurel B. Goodwin
New Mexico Institute of Mining and Technology
Department of Earth and Environmental Science
801 Leroy Place
Socorro, NM 87801

Abstract

Teapot Dome is an asymmetric, doubly plunging, basement-cored, Laramide-age anticline. A systematic study of natural fractures within the Cretaceous Mesaverde Formation at Teapot Dome, Wyoming indicates that lithology and structural position control outcrop fracture patterns. Lithology controls fracture, deformation band and fault patterns in the following ways: 1) fracture intensity increases with increased cementation, 2) fracture spacing increases proportionally with bed thickness within two sandstone facies, but not in carbonaceous shales where fracture spacing is inversely proportional to bed thickness, 3) coal cleats are generally oblique, by up to 20 degrees, to fractures in sandstones, 4) most fractures in sandstone units terminate at contact with shale layers, 5) deformation bands occur almost exclusively in a poorly cemented, high porosity, beach-sand facies, 6) normal faults within well cemented sandstones are generally expressed as fracture zones, whereas the same faults within poorly cemented sandstones are diffuse zones of subparallel deformation bands.

Three primary throughgoing fracture sets were documented within this context. The oldest fracture set is oblique to the hinge of the anticlinal fold. The vast majority of these fractures strike NW to WNW. A small number of these oblique fractures strike roughly NNE. Fractures that strike oblique to the fold hinge appear to predate folding. The other two fracture sets are related to folding. The most common of these fractures, which are found throughout the fold, are bed-normal extension fractures striking subparallel to the fold hinge. A third set consists of bed-normal extension fractures striking perpendicular to the fold hinge. In many areas this fracture set is spatially related and subparallel to NE-striking, normal oblique-slip faults. The normal oblique-slip faults are common along the eastern limb, but more than 90% of these faults terminate before intersecting the western limb. Conjugate fractures, deformation bands and faults, oriented such that they have a vertical bisector to the acute angle and striking subparallel to the axis of the anticline, are common in the southwestern limb and southern arc of

the anticline. Hinge-parallel and hinge-perpendicular fractures and faults are broadly contemporaneous with basement-involved thrusting and folding at Teapot Dome, as suggested by their spatial relationship to the fold. Further observations suggest that fault-related, hinge-perpendicular fractures are generally the same age as hinge-parallel fractures, and NE-striking, normal oblique-slip faults are oriented roughly perpendicular to the fold hinge, even where it bends, and terminate toward the SW limb of the anticline. The oblique movement recorded on some of these NE-striking faults may be related to differential movement across individual segments of the basement-involved thrust.

Based on the Teapot Dome natural fracture data set, a 3-D conceptual model of fractures associated with basement-cored anticlines suggests significant horizontal permeability anisotropy. Depending on structural position, the interaction between fracture sets, and the in situ stress, the direction of maximum permeability can be either parallel or perpendicular to the fold hinge.

Table of Contents

List of Figures

List of Tables

1.0 INTRODUCTION

1.1 Purpose of study

This work was undertaken in order to provide a characterization of the natural fractures within the Mesaverde Formation at Teapot Dome. This report is based on work done for a Master's Thesis at New Mexico Institute of Mining and Technology by the first author (Cooper, 2000). The questions addressed in the report concern the origin, distribution, and orientations of natural fractures and deformation bands and their probable effects on similar hydrocarbon reservoirs. To facilitate discussion of these items this report has been divided into two parts; lithologic controls on fracturing and structural controls on fracturing.

1.2 Location and General Geology

Teapot Dome is located in central Wyoming, near the southwestern edge of the Powder River Basin (Figure 1). The deepest portions of the Powder River Basin contain nearly 5,500 m of sedimentary rocks, approximately 2,440 m of which are nonmarine Upper Cretaceous and lower Tertiary clastic sedimentary rocks related to Laramide orogenesis (Fox et al., 1991). The tectonic style of Laramide uplifts varies around the basin, with the greatest deformation along the western and southern margins. Teapot Dome is one of several productive structural-style hydrocarbon traps associated with Laramide structures in this area and is part of a larger structural complex, comprised of Salt Creek anticline to the north and the Sage Spring Creek and Cole Creek oil fields to the south (Doelger et al., 1993; Gay, 1999). Teapot Dome is similar to other Laramide structures such as Elk Basin anticline and Oil Mountain (Engelder et al., 1997; Hennings et al., 1998; Hennings et al., 2000).

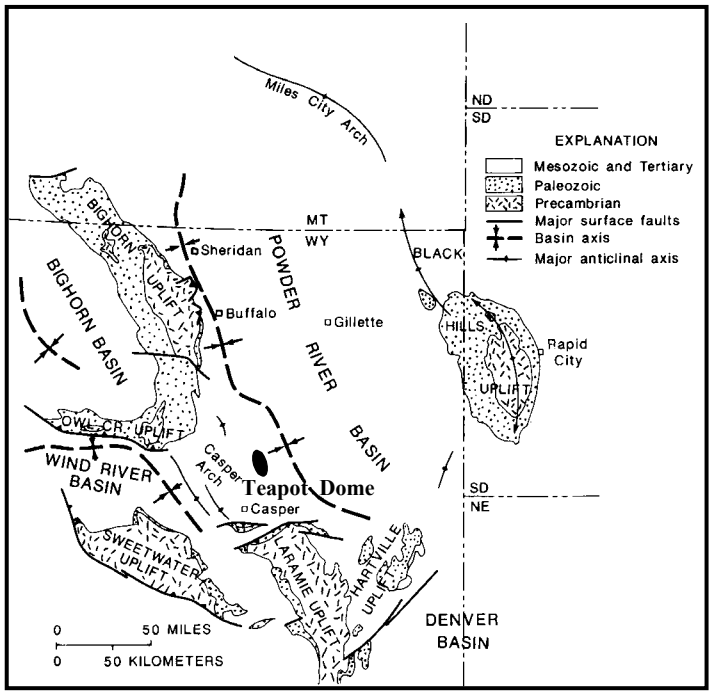

Figure 1: Index map illustrating the general location of Teapot Dome relative to the Powder River Basin and surrounding Laramide uplifts (modified from Fox et al., 1991).

Early debates concerning the deformational style of the Laramide orogeny generally centered around two main models: 1) forced folding related to near vertical uplifts (Prucha et al., 1965; Stearns, 1971; Stearns, 1975; Stearns, 1978) and 2) high-angle reverse faulting related to crustal shortening (Blackstone, 1940; Berg, 1962; Blackstone, 1980). Over time, evidence has accumulated for crustal shortening accommodated in the area of interest (e.g. Wyoming, Montana, and South Dakota) by thrusts, many of which extend into the basement (Willis and Brown, 1993). This evidence includes seismic reflection data (Gries, 1983; Gries and Dyer, 1985) and a deep crustal line across the Wind River Range by COCORP (Oldow et al., 1989). Teapot Dome is typical of the structures formed by this deformation process. At Teapot Dome, a basement-involved thrust that terminates upward within the sedimentary section (Figure 2) is evident in 2-D seismic data (LeBeau, 1996). The dome itself is a doubly plunging anticline. Normal oblique faults that strike predominately perpendicular to the curvilinear fold hinge are common along the eastern limb (Olsen et al., 1993; Doll et al., 1995). Mesaverde Formation sandstones and shales are exposed along the western, eastern and southern limbs of Teapot Dome. Maximum dips along the western limb are near 30^{o}; along the eastern limb dips range from 7^{o} to 14^{o}.

A resistant rim of Mesaverde Formation sandstones is exposed along the eastern, southern and western limbs of Teapot Dome. At this location, the Mesaverde Formation can be subdivided into two members: the Teapot Sandstone Member and the Parkman Sandstone Member (Wegemann, 1918; Thom and Speiker, 1931). The Teapot Sandstone Member overlies the Parkman Sandstone Member with an intervening layer of marine shale. This relationship suggests sea regression during deposition of the Parkman Sandstone Member, followed by a brief transgression, then regression during the deposition of the Teapot Sandstone Member (Weimer, 1960; Zapp and Cobban, 1962; Gill and Cobban, 1966). An unconformity at the base of the Teapot Sandstone Member represents probable subaerial exposure and erosion associated with eustatic sea level change driven by regional tectonism (Gill and Cobban, 1966; Weimer, 1984; Merewether, 1990; Martinsen et al., 1993). Fractures within the Parkman Sandstone Member are the principal focus of this study.

The Steele Shale is exposed at the surface within the central portion of this breached anticline. An exploratory well (No. 1-G-10) near the apex of the anticline encountered granitic basement at a depth of 2084 m (6849 ft; Gribbin, 1952).

The shallowest reservoirs at Teapot Dome are within the Shannon Formation. This formation is also one of the major producing intervals and is located at depths between 75-200m. The sandstones within this formation were deposited as offshore bars along the margin of the Cretaceous Western Interior Seaway (Tillman and Martinsen, 1984). Data from core within the Shannon Sandstone will be addressed in section 2.4.4.

A major set of faults and fractures striking perpendicular to the hinge of the anticline and a secondary set parallel to the fold hinge were recognized and described at Teapot Dome by Thom and Spieker (1931). Thom and Spieker (1931) suggested that these faults and fractures

may inhibit fluid flow if they are cemented, and discussed the possibility of increased hydrocarbon flow if a production well should intersect open fracture zones. However, they suggested that fractures would penetrate both sandstones and shales. If this were the case fractures would allow communication between reservoir units and pressures would equalize. Because different pressures were observed within different reservoirs Thom and Spieker (1931) inferred that fractures did not significantly influence hydrocarbon flow.

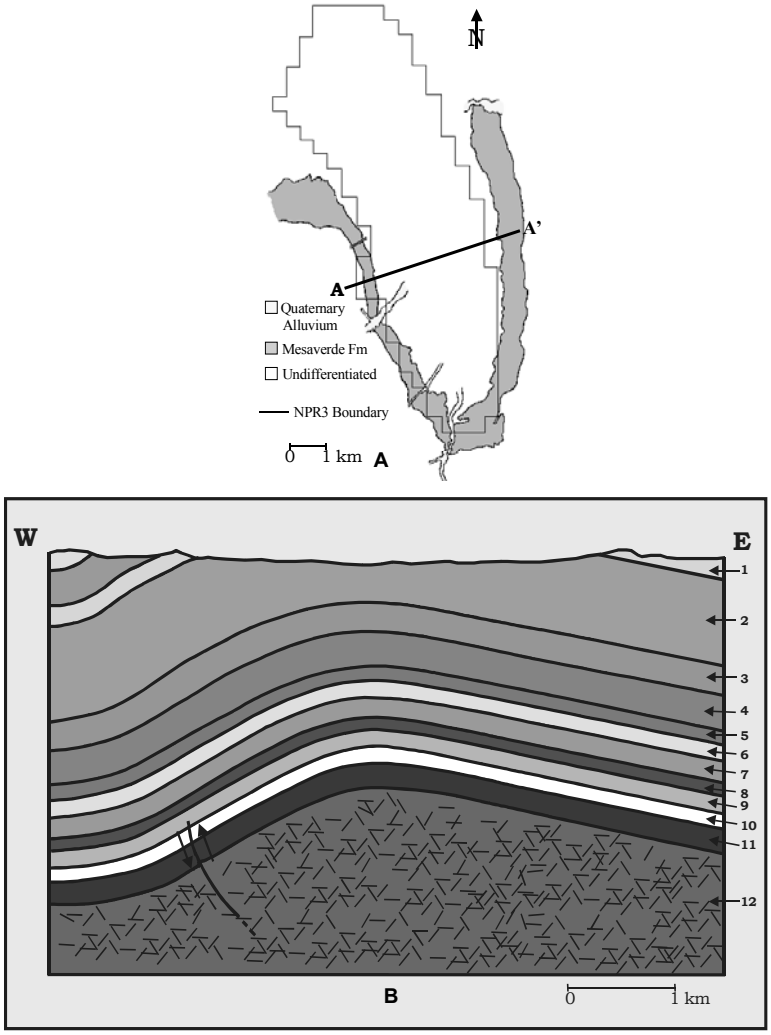

Figure 2: A. Map view of cross section transect. B. Diagrammatic cross section illustrating general structure and the basement-involved thrust that tips out within the sedimentary section. Cross section was constructed from surface data, well logs and 2-D seismic reflection data. No vertical exaggeration. Numbers correlate to the following stratigraphic units and systems as provided from Doll et al. (1995) and from well logs of exploratory well no. 1-G-10: 1. Cretaceous Mesaverde Formation (Fm). 2. Cretaceous Sussex Sandstone (Ss), Shannon Ss, Steele Shale (Sh), Niobrara Sh, Frontier Fm. 3. Cretaceous Mowry Sh, Muddy Ss, Thermopolis Sh, Dakota Ss, Lakota Ss. 4. Jurassic Morrison Fm, Sundance Fm. 5. Triassic Chugwater Group. 6. Permian; Goose Egg Fm. 7. Pennsylvanian Tensleep Ss. 8. Pennsylvanian Amsden Fm. 9. Mississippian Madison Limestone (Ls). 10. Devonian through Ordovician; Undifferentiated. 11. Cambrian; Deadwood Fm. 12. Precambrian; Granite.

Thom and Speiker (1931) also documented a secondary set of faults and joints that strike roughly normal to the major set of faults and fractures and are, therefore, oriented approximately parallel to the axis of the anticline. This subsidiary fracture and fault set was attributed to extension across the fold. Doll et al. (1995) inferred three primary fracture directions in the subsurface from steam flood response data. These orientations were perpendicular to the fold hinge, N65^{o}W, and parallel to the hinge. Using indirect surface geochemical techniques such as surface hydrocarbons, Eh, pH, soil electrical conductivity, iodine, and bacteria, Fausnaugh and LeBeau (1997) observed trends in the data suggesting NE-striking faults. Geochemical signatures perpendicular to the NE-striking faults were also observed and attributed to either faulting or to overlapping stratigraphic relationships of subsurface reservoirs. Section 3 (Structural Controls) describes three dominant fracture patterns observed at Teapot Dome. Two of the fracture sets appear to be related to the folding process and are oriented roughly parallel and perpendicular to the fold hinge. The third set predates folding and predominately strikes WNW.

1.3 Background

Structures such as fractures, fracture networks and faults can influence permeability and therefore fluid flow within an aquifer or petroleum reservoir (Lorenz and Finley, 1989; Lorenz and Finley, 1991; Teufel and Farrell, 1992). A distinct permeability anisotropy has been observed in reservoirs with low matrix permeability and a well developed, open fracture system (Elkins and Skov, 1960; Lorenz and Finley, 1989; Teufel and Farrell, 1992), with the highest permeability parallel to the fractures. Within a given rock volume fractures generally result in an overall permeability increase. Significant interaction between the fracture surface and the matrix allows better drainage of the rock matrix. This matrix/fracture interaction could allow for a substantial increase in recoverable hydrocarbon reserves.

In contrast, mineralized fractures and deformation bands (small-displacement faults, characterized by cataclasis and/or pore reduction through compaction) are typically characterized by significant permeability reduction (Nelson, 1985; Antonellini and Aydin, 1994; Antonellini et al., 1994). Where fractures are mineralized or the rock is cut by deformation bands, the rock matrix is more permeable than the structures, so the rock is most permeable parallel to, and between, fractures and deformation bands. Therefore, within a given rock volume containing mineralized fractures and/or deformation bands there will be an overall permeability decrease and possible reservoir compartmentalization. Partially mineralized fractures may still have some permeability. However, there could be a significant reduction in the interaction between the remaining open fracture fluid pathway and the rock matrix (Nelson, 1985). Either mineralized or partially mineralized fractures could have the effect of decreasing the total amount of recoverable reserves.

Structures such as fractures and faults can increase or decrease permeability in certain directions and thus introduce permeability anisotropy and heterogeneity (Rice, 1983; Nelson, 1985; Fassett, 1991; Teufel and Farrell, 1992; Caine et al., 1996) and it is important, from a production standpoint, that they be modeled accurately. It can be very difficult, however, to

predict the location, spacing, and orientation of fractures and small-displacement faults in the subsurface (Lorenz, 1997). Most regional fractures are subvertical, and are thus unlikely to be sampled in vertical boreholes (Lorenz and Hill, 1992). Reasonable predictions of permeability anisotropy require an understanding of controls on the distribution and orientation of such features. As will be brought out in this report these features can have predictable orientations with regard to large-scale structures such as anticlines.

Basement-cored anticlines within the Rocky Mountain region have been hydrocarbon exploration targets since the turn of the century. Structures of this type can be found in many other areas of the world (e.g., DeSitter, 1964; Harding and Lowell, 1979). One of the primary reasons basement-cored anticlines are exploration targets is that they can provide excellent four-way closure. Four-way closure can allow the entrapment of migrating hydrocarbons in economically significant amounts. To maximize recovery of these trapped hydrocarbons it is essential to accurately model any permeability anisotropy associated with these structures.

For modeling and production purposes it is important to document directions of preferred fracture and fault orientations within primary hydrocarbon traps, such as anticlines. By understanding controls on fracture and fault orientation and distribution in a given reservoir the accuracy of flow modeling can be improved, thereby increasing primary and secondary hydrocarbon recovery. To this end lithologic controls on fracturing as well as some of the consequences of fracture permeability are reviewed in the first part of this report while the second half addresses variations in fracture and fault characteristics, such as spacing and orientation, with structural position.

1.3.1 Historical context

Oil seeps were known to exist in the Teapot Dome and Salt Creek areas prior to 1880. The first oil well in the area was drilled in 1889 near one of the seeps north of the Salt Creek anticline. The well was drilled to a depth of approximately 213 m (700 ft) and had a production of 10-15 barrels per day (b/d) from sand lenses in the Steele Shale (Curry, 1977). Teapot Dome was established as a Naval Petroleum reserve by President Wilson in 1915 (Doll et al., 1995). The first production at Teapot Dome was 830 barrels in October 1922, representing two days of flow (well ID # 301-2; Trexel, 1930). Peak production in 1923 was 138,081 barrels in October from 51 wells or 4460 barrels per day (Trexel, 1930).

The infamous Teapot Dome scandal of the Harding Administration involved leasing of this Government-owned reserve to Harry F. Sinclair's Mammoth Oil Company in 1922. Daily production when placed in the hands of the receivers in 1924 was approximately 3790 barrels per day (b/d). Trexel (1930) provides monthly sales and royalty figures for this period. These data show total oil and gas sold by Mammoth Oil Company was 1,442,496 barrels. Trexel (1930) also indicates that Mammoth Oil produced between 2 and 2.5 billion cubic feet of gas by March 13, 1924. Reports indicate that during this period some shale-crevice wells had production rates as high as 25,000 b/d (Curry, 1977). However, overall production dropped to 22,626 barrels per month by December 1927. Therefore, during the scandal, wells were producing at a maximum rate and much of the reservoir pressure within the Second Wall Creek Sandstone was depleted (Curry, 1977; Doll et al., 1995).

The current manager of Teapot Dome, also known as Naval Petroleum Reserve #3 (NPR #3), is The Department of Energy. Cumulative production for the year 1998 was 250,000 barrels of sweet crude oil, and 26,000 barrels of sour crude oil from an average of 500 production wells (Milliken, pers. com., 1999). NPR#3 is slated for closure and reclamation by 2003. At present one of the major uses of the Teapot Dome Field is as a testing center for new technologies. This research is managed through the Rocky Mountain Oilfield Testing Center located in Casper, Wyoming and on site at Teapot Dome.

1.4 Technical approach

Data collection sites were chosen to provide 1) a generally uniform distribution of sites with regard to the large-scale anticlinal structure, and 2) representative samples from the five different stratigraphic units within the Mesaverde Formation. Data were collected by systematically recording the grain size, degree of cementation, bed thickness, and orientation of a given lithologic unit and the type, orientation, spacing, trace length, degree of mineralization, aperture width, surface characteristics, and abutting relationships of fractures cutting that unit. At certain charted locations the fracture patterns were mapped to scale. These maps help to illustrate the abutting relationships in areas where two or more sets exist. Preference was given to localities that provided a 3-D view (e.g., combined pavement and cross-sectional views).

2.0 LITHOLOGIC CONTROLS

2.1 Introduction

Previous work indicates that lithology and bed thickness are primary controls on fracture spacing and orientation, reflecting the fact that different rock units are mechanically distinct (Nelson, 1985; Fjaer et al., 1992; Committee on Fracture Characterization and Fluid Flow, 1997; Lorenz, 1997). Fracture spacing (also referred to as fracture density) has been correlated with the mineralogical composition of the matrix grains, porosity, and bed thickness. In general, more brittle rocks will have more closely spaced fractures than less brittle rocks (Nelson, 1985). Therefore, rock units that contain high percentages of well-cemented brittle constituents will generally have more closely spaced fractures. The primary brittle constituents within a rock are quartz, feldspar, dolomite and calcite. However, it should be noted that the elastic properties of a given rock unit, which have a direct influence upon fracture spacing, need not always be associated with the amount of brittle constituents. For example cleat or fracture spacing within carbonaceous shales and coals with few quartz grains is in many cases much closer than the fracture spacing within quartz-rich sandstone beds of similar thickness (Price, 1966). This suggests that the difference in fracture spacing is more directly attributed to Young's modulus than to brittle constituents.

It has also been observed that when loading conditions and all other rock parameters are equal, thin beds will have a higher fracture density than thicker beds (Price, 1966; Ladeira and Price, 1981; Nelson, 1985). With a few exceptions fracture spacing is locally proportional to bed thickness (Price, 1966; Hobbs, 1967; Nelson, 1985; Lorenz et al., 1996).

Examination of natural fracture and fault patterns within Mesaverde Formation outcrops at Teapot Dome, Wyoming was undertaken, in part, to develop a better understanding of the influence of lithology and bed thickness on the development of these structures. Additional work (presented in section 3: Structural Controls) addresses variations in fault and fracture density and orientation with respect to structural position within the dome. Together, these two studies provide insight into controls on deformation of a heterogeneous sequence of clastic sedimentary rocks in a basement-cored anticline.

2.2 Previous Work

2.2.2 Lithologic Controls on Fracturing

Fracture spacing is generally proportional to bed thickness (Bogdanov, 1947; Harris et al., 1960; Price, 1966; McQuillan, 1973; Narr and Suppe, 1991; Gross, 1993; Ji and Saruwatari, 1998; Bai and Pollard, 2000). Bai and Pollard (2000) evaluated previous studies and showed that spacing to layer thickness ratios range from greater than 10 to less than 0.1. Bogdanov (1947) mathematically described a relationship where spacing (S) varied as a function of bed thickness (B) and some constant (K). The constant (K) has been related to lithology (Ladeira and Price, 1981).

Equation 1: $S = K B$

Price (1966) attributed differences in spacing between fractures in a sandstone and coal cleats in an adjacent carbonaceous unit to differences in Young's modulus. In beds of similar thickness and within the same area, coal cleat spacing can be less than 3 cm whereas fracture spacing within sandstone can be over 35 cm. In evaluating this relationship, Price (1966) equated strain energy (w) to the applied stress (σ) and Young's modulus (E):

Equation 2: $w = \sigma^2 / 2E$

Given generalized Young's moduli of $E= 2 \times 10^5$ and $E = 1 \times 10^7$ for coal and sandstone, respectively, the strain energy stored in the carbonaceous unit can be several times that of the sandstone. The difference in stored strain energy is the same order of magnitude as the difference in fracture spacing.

With respect to fracture spacing within a single bed Price (1966) suggests that at some distance L from a preexisting fracture forces become large enough to form a second fracture. Therefore L is the limit of influence of the preexisting fracture and is the minimum distance at which a second fracture can be formed. Further, if bed thickness is doubled, a distance of 2L is required for the forces to become large enough to form a second fracture. Essentially Price (1966) implies a linear relationship between bed thickness and fracture spacing. Harris et al. (1960) suggests that fracture density is nearly the inverse of bed thickness. However, bed orientation, thickness of cover, and the degree of cohesion between adjacent units all influence normal stress on the rock units. Also small lithologic changes, such as grain size, sorting and cementation, will influence both tensile strength and the coefficient of friction (Price, 1966). Price (1966) suggested these mitigating factors produce only second-order fluctuations in the bed

thickness to fracture spacing relationship. Other workers (Lorenz and Finley, 1989; Lorenz and Hill, 1991; Lorenz, 1997) have observed that lithologic changes and sedimentary heterogeneities, such as grain composition, cementation and orientation of lenticular fluvial sandbodies relative to the stress field, can influence mechanical behavior and have a visible effect on fracture distribution and spacing.

Fracture spacing has also been related to the rock properties and thickness of the adjacent rock units as well as the rock properties of the fractured bed (Ladeira and Price, 1981; Ji and Saruwatari, 1998; Bai and Pollard, 2000). Hobbs (1967) suggested that fracture spacing is proportional to the square root of Young's modulus for the fractured bed and the inverse of the square root of the neighboring units' shear moduli. Ji and Saruwatari (1998) devised a mathematical model to describe a fractured bed interlayered between two unfractured beds. In the model fracture spacing (s) depends on the fractured layer thickness (t) and the surrounding non-fractured layer thickness (d).

Equation 3: $s = n\,(td)^{1/2}$

The constant n is dependent on material properties of the rock units and the decay modes of the shear stress in the bounding layers. The model is supported by field data from Ladeira and Price (1981).

Methods of evaluating layer thickness to fracture spacing include the Fracture Spacing Index (Narr and Suppe, 1991), Fracture Spacing Ratio (Gross, 1993) and Fracture Spacing to Layer Thickness Ratio (Bai and Pollard, 2000). The Fracture Spacing Index (FSI) is the slope of a best-fit line through the origin on plots of mechanical layer thickness vs. median fracture spacing from a number of layers of varying thickness. In these plots thickness is on the y-axis however fracture spacing is held as the dependent variable. The plots are arranged in this manner so that FSI values correlate to higher fracture density. The Fracture Spacing Ratio (FSR) is the ratio of median fracture spacing vs. layer thickness for a single layer. Bai and Pollard (2000) use the Spacing to Layer Thickness Ratio (S/T_f) as the inverse of either of the two previous measures assuming equal spacing (i.e. mean and median spacing values are the same). Mean rather than median fracture spacing has also been described as directly proportional to bed thickness (Huang and Angelier, 1989). The Spacing to Layer Thickness Ratio was used by Bai and Pollard (2000) because they wished to focus on "fracture spacing rather than on fracture density".

2.2.3 Influence of Porosity on Deformation Processes

Rock strength has generally been shown to decrease in a nonlinear fashion with increasing porosity (Price, 1966; Dunn et al., 1973; Hoshino, 1974). Therefore, the breaking or fracturing strength of clastic sedimentary rocks is closely related to porosity. Hoshino (1974) derived an empirical relationship between rock strength and porosity:

Equation 4: $n = A\,e^{-b\sigma s}$

Where rock strength (σ_s) is proportional to porosity (n). A is the porosity at strength zero and b is related to the amount of strength change for a specific change in porosity. Dunn et al. (1973) expressed this relationship as:

Equation 5: $y = a\, n^b$

where y is the stress difference at failure, n equals porosity, constants $a > 0 > b$ and "through-going fractures develop by coalescence of grain-boundary cracks, porosity and extension fractures". In the case of low porosity rocks, where there is limited open pore space, a through-going fracture will consist primarily or exclusively of linked extension fractures and grain boundary cracks. Therefore, low-porosity rocks are relatively strong because extension fractures must propagate through a relatively large number of grains within a given volume. In contrast, rocks of higher porosity have numerous open pore spaces, which requires fewer grains to be fractured. As through-going fractures develop, they will use open pore spaces whenever possible because crack propagation in this way requires the least energy (Dunn et al., 1973).

High porosity sandstones commonly deform by a mechanism different than less porous, more brittle sandstones. Deformation within relatively high porosity sandstones can occur by a combination of sand grain fragmentation and pore collapse localized within very narrow bands accommodating displacements of a few millimeters to centimeters (Engelder, 1974; Aydin, 1978; Jamison and Stearns, 1982; Antonellini et al., 1994). These generally planar small-displacement faults are defined as deformation bands (Aydin, 1978). They are typically thin (1mm wide average) with along strike lengths from a few centimeters to some tens of meters in length. Three major groups of these small-displacement faults have been described (Antonellini et al., 1994): 1) deformation bands with no cataclasis, 2) deformation bands with cataclasis and 3) deformation bands with clay smearing. Formation of deformation bands of the first group is believed to be the result of early, transient dilatancy during grain boundary sliding. This can be followed by the formation of deformation bands of the second group through grain breakage and pore collapse. The rotation and crushing of grains results in reduced permeability relative to the surrounding matrix (Antonellini et al., 1994). Experimental analyses indicate that the effective pressure required for failure at the transition between brittle faulting and cataclastic flow in porous sandstones decreases with increasing porosity and grain size (Wong et al., 1997). This observation is in accordance with field and experimental observations that porous sandstones tend to be less brittle and fail through a combination of early dilatancy, then pore collapse and grain fragmentation (Wong et al., 1992; Antonellini et al., 1994; Wong et al., 1997; Wong, 1998). There is a direct relationship between grain size and deformation band width. This relationship is generally described as linear, with the thickness of deformation bands as some multiple (5-15) of average grain diameter (Roscoe, 1970; Muhlhaus and Vardoulakis, 1988; Antonellini et al., 1994).

2.3 Teapot Dome

2.3.1 Mesaverde Formation Mechanical Stratigraphy

As previously described, early workers (Wegemann, 1918; Thom and Speiker, 1931) subdivided the Mesaverde Formation at Teapot Dome into two members: the Parkman Sandstone

Member and the Teapot Sandstone Member. For this study, a different approach was utilized. The Parkman Sandstone Member was divided into five units according to lithology and depositional environment. These divisions best create units with inherently different mechanical properties. Separating units according to mechanical properties is important due to mechanical influences on fracture characteristics. The majority of the fracture measurements were obtained from these five newly defined lithologic units within the Parkman Sandstone Member. From oldest to youngest, these units are a shallow-marine, interbedded sandstone/shale, shoreface/beach sandstone, a white beach sandstone, a non-marine carbonaceous shale, and lenticular fluvial sandstones within the carbonaceous shale unit. A generalized stratigraphic column is provided in Figure 2. The stratigraphic sections allow consideration of spatial variations in thickness as well as facies variations within the units studied. Key observations and justifications for the environments of deposition within this progradational sequence are summarized in the following paragraphs.

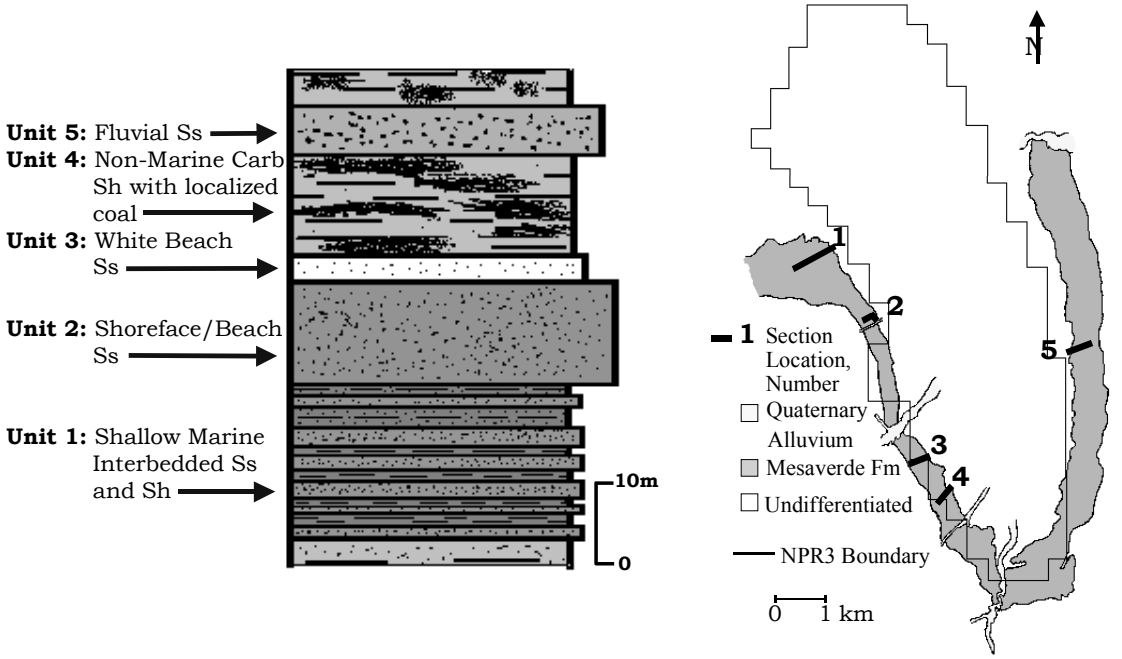

Figure 3: Generalized stratigraphic column based on measured sections illustrating the relative positions and thicknesses of the five Parkman Sandstone Member stratigraphic units from which fracture orientation data were recorded at Teapot Dome. Locations of measured sections are shown in the map view.

Unit 1 consists of interbedded shallow-marine sandstones and shales and ranges in thickness from 10 to 20 m, with individual bed thicknesses from 2 cm to 150 cm. This unit is similar to a basal unit described by Thom and Spieker (1931). This unit is thicker in the northern half of the anticline. Grain sizes coarsen upward from 62-125 μ in the lower sandstones to 88-177 μ in the upper beds. The alternating beds of shale and sandstone, numerous trace fossils, current ripples and occasional hummocky cross-stratified beds found within this unit are evidence that these sandstones were deposited in a shallow-marine environment near wave base. When below wave base, the clay was deposited and not reworked/redistributed farther offshore into the deeper marine environments. When above wave base, sands were reworked into

hummocky cross-stratified beds. Reworking was intermittent because trace fossils and current ripples were not always destroyed before burial.

The shoreface/beach sandstone unit (Unit 2) has an average thickness of 15-20 m. Grain sizes average between 88 and 177 μ. The thickest portion of this unit is found along the southeastern extent of the anticline (up to 20m thick). The basal (transitional) portion of this unit locally displays rip-up clasts, ball, pillow and flame primary structures, and *Ophiomorpha* trace fossils. The lack of trace fossils (except for the armored *Ophiomorpha* burrows) indicates that these deposits were shallow enough for constant reworking by wave and storm processes. Half-meter scale unidirectional crossbedding is suggestive of long-shore currents and offshore bars. Thicker sandstone beds with fewer and thinner shale beds relative to the shallow-marine facies suggest stronger shoreface currents during transport. The ball and pillow structures may represent rapidly deposited sandstones. The sands could be derived from surging currents directed offshore, after storms flooded low-lying coastal areas. Alternatively, these structures could be related to synsedimentary earthquake activity (Kuenen, 1958; Potter and Pettijohn, 1977).

The white beach sandstone unit (Unit 3) is distinctive due to its snowy white color, higher porosity and lesser amount of cementation relative to any of the other Mesaverde Formation sandstones. Thom and Spieker (1931) also described this unit. This unit is absent along the northwestern portion of the dome, is present as a thin (up to 2 m) unit along the western and southern portions, and thickens to a maximum of 4.5 m along the eastern limb of the anticline. Grain sizes are between 125 and 250 μ. While sedimentary structures in this unit are typically obscure, carbonaceous shales deposited in paludal/swamp environments directly overlie it, suggesting this unit represents the bedding deposits expected between shallow marine and paludal environments.

The non-marine carbonaceous shale (Unit 4) averages 40 m in thickness and is locally interbedded with thin coals. A distinctive black color, generally poor induration, and a very fine grain size (less than 62 μ) characterize this unit. These organic-rich carbonaceous shales are indicative of swampy environments. There are no distinct paleosols or rooted zones to indicate subaerial exposure. However, there are pieces of fossilized wood as well as twig/leaf imprints in the rock.

Laterally discontinuous, over a scale of 10s of meters, fluvial sandstones (Unit 5) are located within the carbonaceous shale unit. For the purposes of this study, fluvial sandstones are treated separately from the carbonaceous shales because of significant differences in grain size and cementation (and therefore inferred differences in mechanical properties). Unlike the other stratigraphic units, which have a tabular or sheeted geometry, the fluvial sandstones are lenticular. Individual fluvial sandstone units range between 1 and 6 m in thickness. Sandstone lenses are generally poorly sorted with grain sizes varying between 88 and 250 μ. Crossbeds are generally uniformly oriented at any single outcrop, but are variable from channel to channel or from location to location along a channel, reflecting channel sinuosity. Associated ripple-bedded, finer-grained, thin-bedded overbank and levee deposits occur lateral to the channels or overlie the channel deposits. In the later case these deposits may have formed during channel

abandonment.

2.4 Fractures and Faults at Teapot Dome

The dominant type of fractures observed at Teapot Dome are extension fractures that are primarily oriented parallel or perpendicular to the fold hinge (see Section 3: Structural Controls). At most sample locations there are multiple fracture sets, including throughgoing fractures and cross fractures (Figure 4). The majority of apertures measured at these locations are the result of recent erosion and thus are not discussed here. Surface features such as plume and rib structures were noticeably absent on almost all exposed throughgoing fracture surfaces. Due to the limited size of outcrop exposures, fracture trace length data were generally unobtainable at Teapot Dome. The throughgoing fractures generally extended from outcrop edge to outcrop edge. Fracture zones in one large pavement surface, within Unit 2 beach sandstones, extend over 100m along strike.

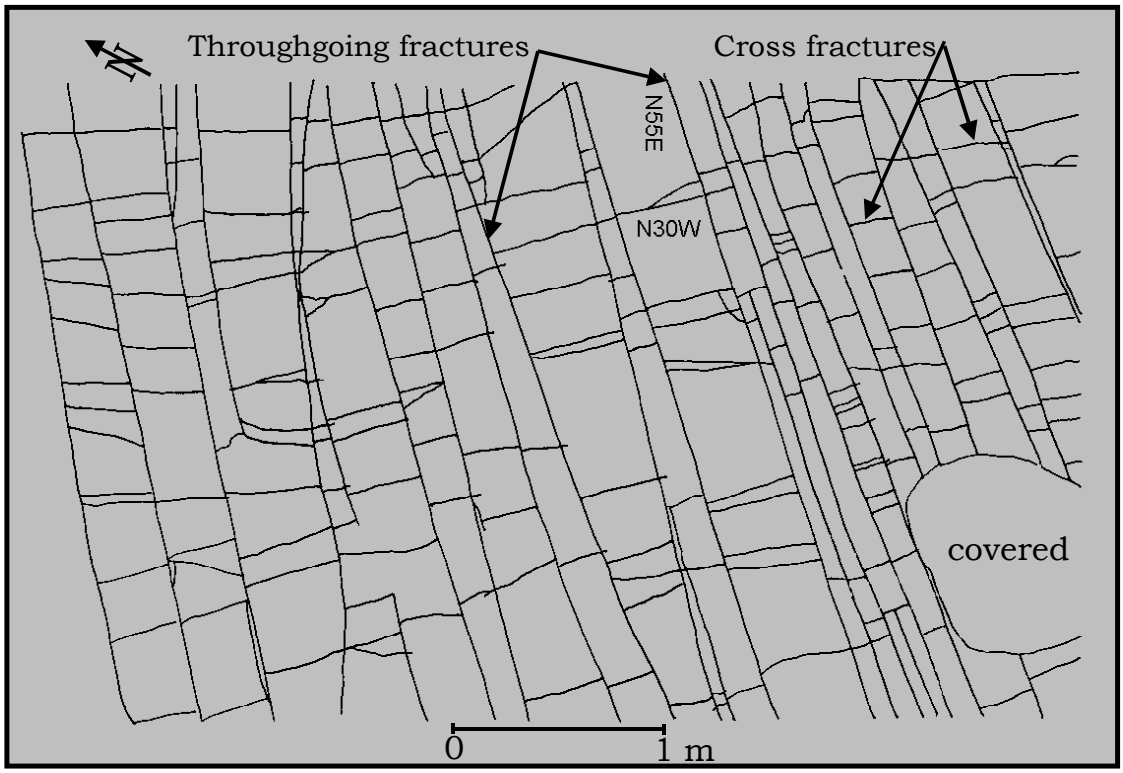

Figure 4: Fracture map of a pavement surface illustrating the nature of throughgoing fractures and cross fractures at the top of a single sandstone bed at Teapot Dome, Wyoming.

2.4.1 Lithologic Controls

Both fracture spacing and orientation vary with lithology at Teapot Dome. In general, fractures are most closely spaced in carbonaceous shales (Unit 4), more widely spaced in fluvial (Unit 5) and beach (Unit 2) sands, and most widely spaced in marine shales (Unit 1). Fractures are generally absent, replaced by deformation bands, within the white beach sandstones of Unit

3. Details of these relationships follow.

Unit 1 marine shales exhibit fewer fractures than associated well cemented Unit 1 marine sandstones. In general, regional fractures in the sandstones terminate at sandstone/shale contacts, but this fracture-termination relationship was observed everywhere Unit 1 was investigated. Unit 4 carbonaceous shales with localized coal seams have a relatively high cleat (extension fracture) density that in many areas is comparable to or greater than the fracture density within well cemented sandstone beds of similar thickness (Figure 5). For example, two distinct fracture sets are observed within the Unit 2 sandstone, each with a unique orientation and mean spacing of fractures. The NW-striking fracture set has a mean fracture spacing of 29.5 cm, while the NE-striking fracture set has a mean fracture spacing of 185.5 cm. The mean spacing between NW-striking cleats in the Unit 4 carbonaceous shale is 17.2 cm. Comparing the NW-

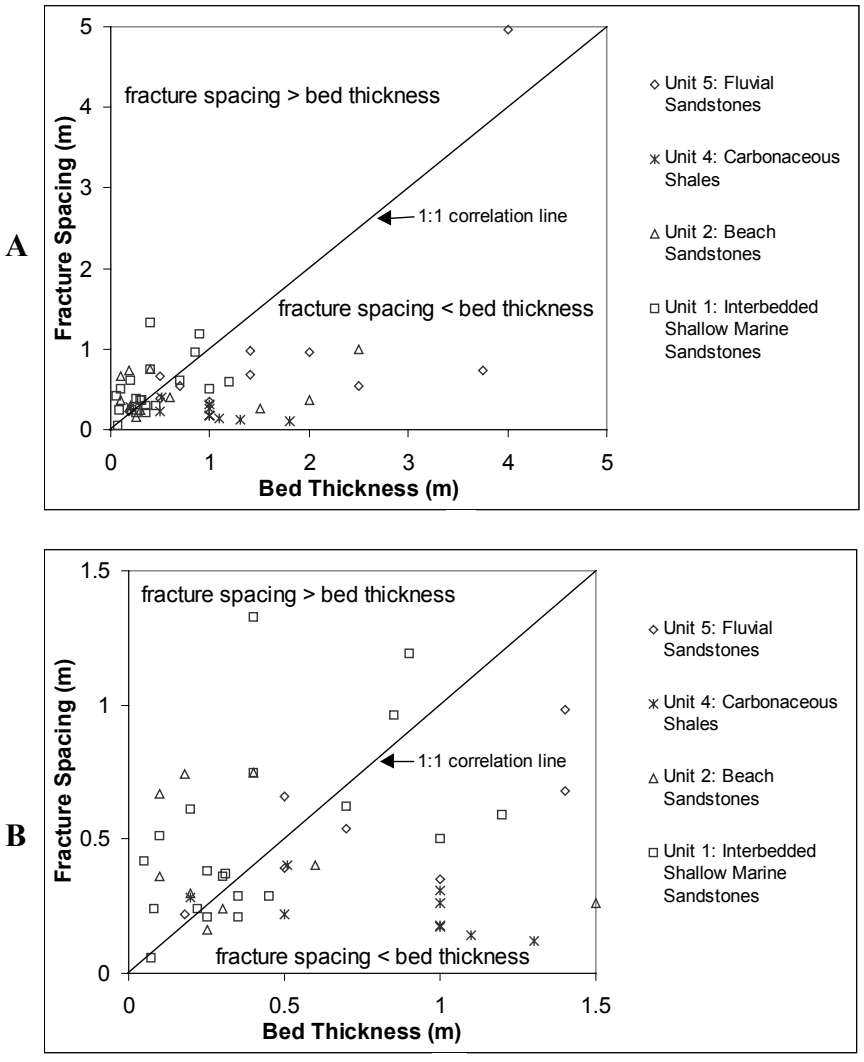

striking fracture set with NW-striking cleat set gives a ratio of cleats to fractures of 1.7:1. This is consistent with Price's (1966) observations of fracture density in coal vs. sandstone.

Figure 5: Fracture spacing vs. bed thickness data from 53 locations and 4 lithologic units around Teapot Dome. Locations were selected on the criterion of at least one distinctly older throughgoing fracture set. Fracture spacing was measured perpendicular to the throughgoing

fracture set and averaged for each location. 594 total fracture spacing measurements were used. Complete fracture and bed thickness data are provided in the appendix of Cooper (2000). (A) All data points are shown. (B) Shows data for bed thickness and fracture spacing values below 1.5m.

A further comparison suggests a significant difference in orientation between fractures and cleats. Fractures are oblique to cleats by up to 20^{o} within beds of similar thickness and relatively close proximity.

Given sandstone beds of similar thickness, fractures are more closely spaced within better-cemented sandstones. Measurements obtained from seven adjacent sandstone beds within Unit 2 illustrate the relationship between the amount of cementation and fracture spacing in sandstones observed throughout Teapot Dome (Figure 6). Fracture spacing of the oldest throughgoing set was measured perpendicular to fracture strike. The oldest throughgoing set at this location is oblique to the fold hinge and has a representative orientation of N55^{o}W 75^{o}NE. Note that porosity is inversely related to the amount of cementation within a specific rock unit (Table 1).

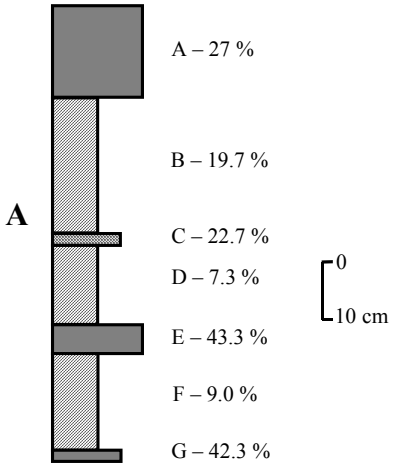

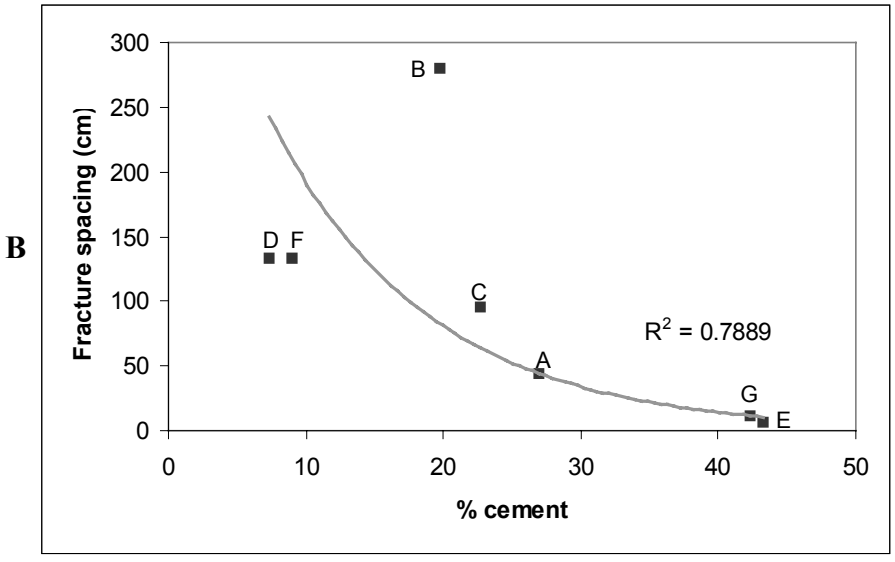

Figure 6: A) Stratigraphic section of seven beds (labeled A, B, C, D, E, F and G) composed of shoreface/beach sandstones within Unit 2. B) Fracture spacing is shown to decrease nonlinearly with increased cementation in a comparison of the same seven beds. Cement percentages were determined from thin section point count data. Fracture spacing is average of measurements from each bed (Table 1). Data table provided in Cooper (2000).

Bed	**A**	**B**	**C**	**D**	**E**	**F**	**G**
Number of measurements	11	1	4	3	61	3	40
Mean Fracture Spacing (cm)	43.6	280.0	95.3	133.3	6.2	133.7	11.3
Cement (%)	27	20	23	7	43	9	42
Porosity (%)	18	39	27	36	5	31	11
Bed Thickness (cm)	16	24	4	14	5	17	2

Table 1: Data illustrating the relationship between fracture spacing, cementation, porosity and bed thickness compiled from seven beds within Unit 2 sandstones (stratigraphic section shown in Figure 6A). Note that porosity is inversely related to cementation. Cementation and porosity measurements are from point counts; 300 points per thin section. Cement is typically calcite with minor amounts of siderite.

2.4.1.1 Bed Thickness

Data from Figure 6 were subdivided by lithology in order to evaluate the common belief that fracture spacing is proportional to bed thickness. Locations with bed normal extension fractures that have unambiguous abutting relationships and are not related to faulting are used in Figures 5 and 7. Only the spacing between fractures in the oldest through-going fracture sets was plotted. This eliminated the necessity of determining the influence of pre-existing fractures on secondary fracture spacing. These data suggest that there is a broad linear relationship as described by Bai and Pollard (2000).

It is important to consider that bed thickness may or may not be the effective mechanical thickness. Gross (1993) defines a lithology-controlled mechanical layer as having boundaries where lithologic variation produces distinctly different mechanical properties, so that the layer will respond homogeneously to an applied force. Effective bed thickness is a term used within this paper to describe the total thickness of adjoining stratigraphic units that respond to a deformation process as a single mechanical unit. Therefore, at Teapot Dome, poor correlation coefficients could be attributed to differences between measured bed thickness and effective bed thickness (Figure 7).

When evaluating Figures 5 and 7 it is important to consider the possible mechanical stratigraphic controls on the various units. For example, marine sandsheets separated by shale (shale/sandstone/shale) may be mechanically different than a contiguous sequence of sandstone beds. Unit 1 sandstones are interbedded in shale. They are laterally continuous shallow-marine sandsheets that have a tabular or sheeted geometry. Unit 2 includes beach sandstones generally interbedded within other beach sandstones. These sandstones have a tabular geometry and are laterally continuous. Unit 4 is laterally continuous and is composed of poorly indurated carbonaceous shales and coal. Unit 5 fluvial sandstones have a lenticular geometry and are laterally discontinuous over a scale of 10's of meters. These fluvial sandstones are interbedded

with carbonaceous shales.

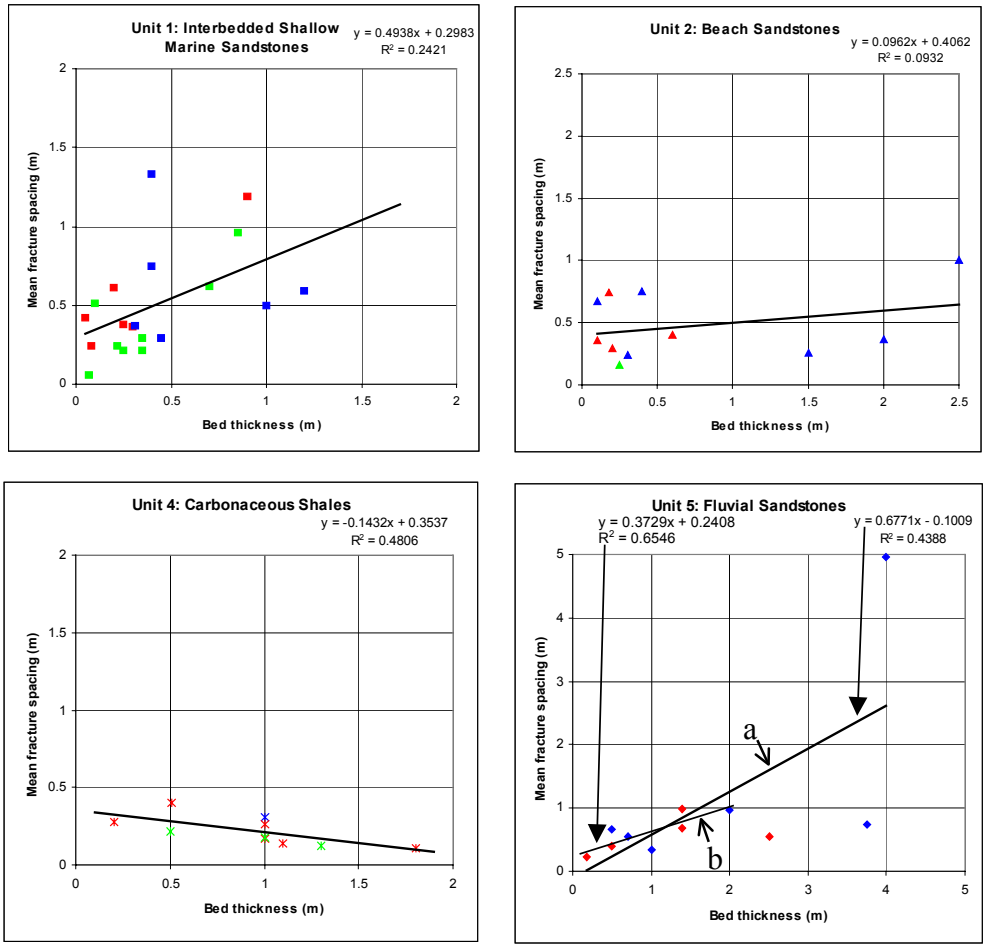

Color Key:
Blue Hinge-parallel fracture set
Green Hinge-perpendicular fracture set
Red Hinge-oblique fracture set

Figure 7: Bed thickness vs. fracture spacing from 53 locations and 4 lithologic units around Teapot Dome. Locations were selected on the criterion that there is at least one throughgoing fracture set. Fracture spacing was measured perpendicular to the throughgoing fracture set and averaged for each location. 594 total fracture spacing measurements were used. There are two fracture spacing vs. bed thickness correlations for Unit 5 fluvial sandstones a) includes all data points and b) a correlation that is minus the three thickest beds. This is the same data set used in Figure 5. Mean fracture spacing is the dependent variable in all three linear regression analyses.

The sandstone units have a variety of bed thickness to fracture spacing relationships. Unit 5 fluvial sandstones have a fracture to bed thickness relationship closest to a 1:1 correlation line (Figure 5). Though the correlation coefficient is poor ($r^2 = 0.4388$), Figure 7 does illustrate a broad positive linear relationship between fracture spacing and bed thickness within Unit 5 sandstones. Ladeira and Price (1981) and Huang and Angelier (1988) indicate that the linear correlation between fracture spacing and bed thickness is no longer observed after beds become a few meters thick. If the three thickest beds are removed from the Unit 5 analysis, a correlation coefficient of 0.6546 is recorded and the equation of the line indicates predicted fracture spacing is approximately 1/3 bed thickness (Figure 7).

The spacing between cleats within Unit 4 carbonaceous shales is inversely proportional to bed thickness (Figures 5 and 7). The correlation coefficient for the Unit 4 linear regression is still poor at 0.4806. Fracture spacing within Unit 2 is the most variable with respect to bed thickness of all the units ($r^2 = 0.2421$; Figure 7).

Unit 1 shallow marine sandstones at first glance show almost no correlation between fracture spacing and bed thickness (Figures 5 and 7). However, the data in Figure 7 are subdivided by orientation of the measured fracture set, and a review of these data shows that hinge-perpendicular fractures within Unit 1 sandstones are better correlated to bed thickness ($r^2 = 0.6719$; Figure 8) than other fractures. This may be due to Unit 1 sandstones being interbedded with an incompetent (shale) layer and thereby creating the condition wherein bed thickness is equivalent to effective bed thickness. Evaluation of fracture orientations within the remaining lithologic units suggests that better correlation coefficients could be obtained once broken into specific fracture sets. However, breaking the data down into smaller segments (i.e. into fracture sets) can increase the correlation coefficient simply because there are fewer data points relative to the initial data set.

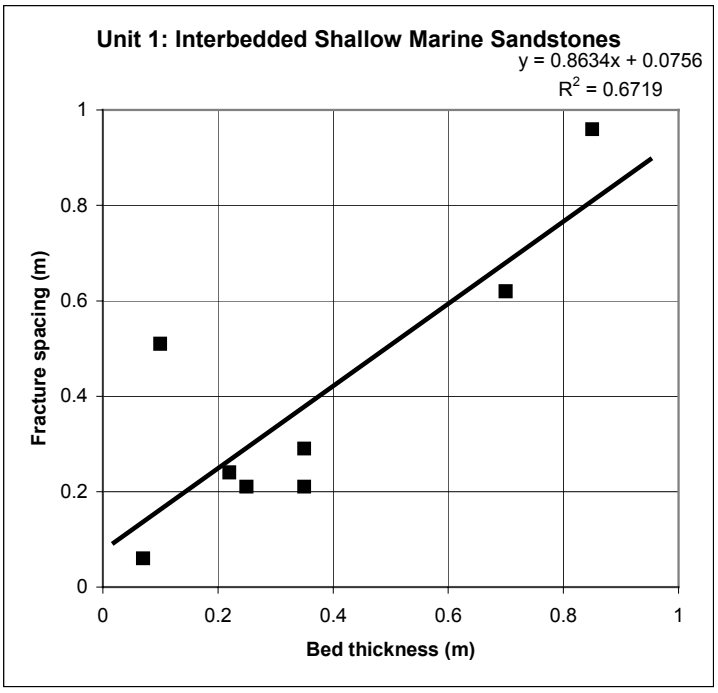

Figure 8: Spacing vs. bed thickness chart for the fracture set oriented perpendicular to the fold hinge within Unit 1 sandstones. This is the same data set as provided in Figure 7 for Unit 1 sandstones minus the other two primary fracture orientations (i.e. parallel and oblique to the fold hinge).

Preexisting fracture sets may affect the spacing of younger fracture sets. For this analysis, the data were subdivided in to the oldest throughgoing set, younger throughgoing sets and cross fractures. Cross fractures strike nearly perpendicular to throughgoing fractures and terminate at intersection with throughgoing fractures. Younger throughgoing fractures can strike

oblique or perpendicular to older throughgoing fracture sets. Younger throughgoing fracture sets can extend through points of intersection with an older set. However, after some distance, the younger set will terminate at intersection with an older throughgoing fracture set. In general fracture spacing is greater in younger throughgoing fractures than in the oldest throughgoing fracture set (Figure 9a). Specifically, a sampling of 23 locations which have two throughgoing fracture sets indicates that at 16 locations the younger set is more widely spaced than the older set (Figure 9a).

A comparison of spacing of cross (i.e. fractures which terminate at throughgoing fractures) to spacing of the oldest throughgoing set indicates cross fracture spacing is greater at 12 out of 16 locations (Figure 9b). If an outlying data point (4.96,4) is not used in the regression analysis, a correlation coefficient of 0.6225 is obtained. Indicating there is a reasonable linear correlation between the two fracture sets of differing age. Within this context younger fractures (i.e. cross fractures) have a wider spacing than older fractures (i.e. throughgoing fractures). Given that cross fractures terminate at throughgoing fractures and that there is a linear spacing relationship between these two fracture sets, cross fracture growth may be controlled by the preexisting fracture set.

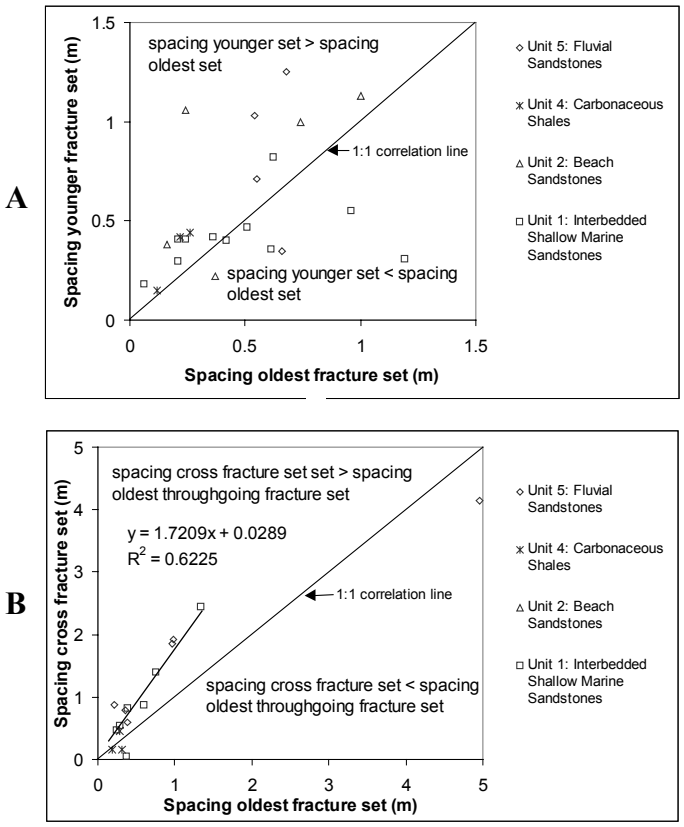

Figure 9: (A) Fracture spacing of a younger throughgoing fracture set vs. fracture spacing of the oldest throughgoing fracture set. The younger set has generally more widely spaced fractures than the older set. (B) Spacing of cross fractures vs. spacing of the oldest throughgoing fracture set. Cross fractures are generally more widely spaced. Cross fractures were modeled as the dependent variable in the linear regression. One outlying data point at (4.96,4) was withheld from the regression analysis.

2.4.1.2 Porosity

One-millimeter wide deformation bands are common in the high porosity, poorly cemented sandstones of the Unit 3 white beach facies (Unit 3: Figure 10). Point count data from four thin sections at two locations within Unit 3 indicate that the rock matrix has an average porosity of 38% at one site and 41% at the second site (Table 2). Average cementation within the matrix is less than 1% at both sites with only minor amounts of iron and/or chert as the primary cements (Table 2).

A comparison of this information with the cementation and porosity data supplied in Table 1-1 for seven sandstone beds within Unit 2 indicates that cementation may be more important than porosity in determining whether a unit deforms through fracturing or formation of deformation bands. Porosities within the Unit 2 sandstones ranged from 5-39% while cementation ranged between 9 and 43% while porosities in Unit 3 sandstones range between 38 and 41% and cementation is below 1%. Therefore, some of the porosity values are similar but the cementation values are at least an order of magnitude higher in the Unit 2 sandstones.

The point count data for Unit 3 sandstones described above can also be used for comparing the physical characteristics of the rock matrix to those of the deformation bands. These data suggest that the deformation bands are composed of crushed sand grains within roughly planar margins (Table 2; Figure 10). The rock matrix has an average porosity of 38% at site 1 and 41% at site 2. Point counts within deformation bands and within the same thin sections indicates average porosity is 5% within deformation bands at sites 1 and 2 (Table 2). This is almost a ten-fold reduction in porosity from the matrix. Average cementation (iron and chert) within the matrix is 1% at site 1 and site 2. The deformation bands at both sites have no measurable cement content. Undifferentiated clay-sized material is abundant within the deformation bands, but is absent from the matrix. Deformation bands at site 1 are composed of 30% clay-sized material on average while deformation bands at site 2 include an average of 23% of this material.

At five locations, deformation bands were recorded within lithologic units other than Unit 3. Two locations are within Unit 5 fluvial sandstones and three are within Unit 2 sandstones. Four of these units were observed in the field to be poorly cemented. The field criterion for a poorly cemented sandstone is that it be friable, easily cut with a knife. Deformation bands and fractures where found together at four of these locations. At one of these locations, two beds of differing cementation within Unit 2 sandstones were recorded. The upper unit was better cemented and contained a majority of the fractures. These fractures typically terminated at the boundary with the underlying poorly cemented sandstone. At two of the sites, deformation bands were parallel to fractures. At a single Unit 2 site, the deformation bands were nearly perpendicular to the throughgoing fracture set and terminated at intersection with the fracture set. Therefore, at this site the deformation bands post-date fracture formation. Age of the deformation bands relative to fractures at the other sites is undetermined.

Field observations of differential iron staining, related to fluid/groundwater flow, indicate that iron may be reduced on one side of a deformation band, but oxidized on the other

(Figure 11). It is evident from petrographic study that deformation bands have a lower porosity relative than the surrounding matrix (Figure 10; Table 2) due to grain breakage and pore collapse. These observations suggest that deformation bands are partial barriers to ground water flow.

A: Unit 3 - matrix

Sample number	1a	1b	2a	2b
Quartz (monocrystaline)	49	58	36	40
Quartz (polycrystaline)	1	trace	6	4
Chert and lithic fragments	7	5	15	12
Feldspar	1	0	2	1
Muscovite	0	1	trace	0
Undifferentiated clay size material	0	0	0	0
Cement (Fe)	0	0	1	2
Cement (calcite)	0	0	0	0
Cement (chert)	0	2	0	0
Macroporosity (intergranular)	35	28	34	36
Macroporosity (intragranular)	1	1	3	2
Microporosity (intragranular)	5	4	3	3
Microporosity (cement)	1	1	1	1
Number of point counts	300	300	300	300

B: Unit 3 - deformation bands

Sample number	1a	1b	2a	2b
Quartz (monocrystaline)	48	68	77	67
Quartz (polycrystaline)	4	1	2	2
Chert and lithic fragments	9	2	4	3
Feldspar	1	0	0	0
Muscovite	0	0	0	1
Undifferentiated clay size material	33	27	20	25
Cement (Fe)	0	0	0	0
Cement (calcite)	0	0	0	0
Cement (chert)	0	0	0	0
Macroporosity (intergranular)	3	2	5	1
Macroporosity (intragranular)	0	0	0	1
Microporosity (intragranular)	1	0	0	0
Microporosity (undifferentiated clay size material)	3	2	2	2
Number of point counts	200	155	108	200

Table 2: Normalized thin section point count data illustrating the differences in porosity, cementation and composition between matrix (A) and deformation bands (B) within Unit 3 sandstones.

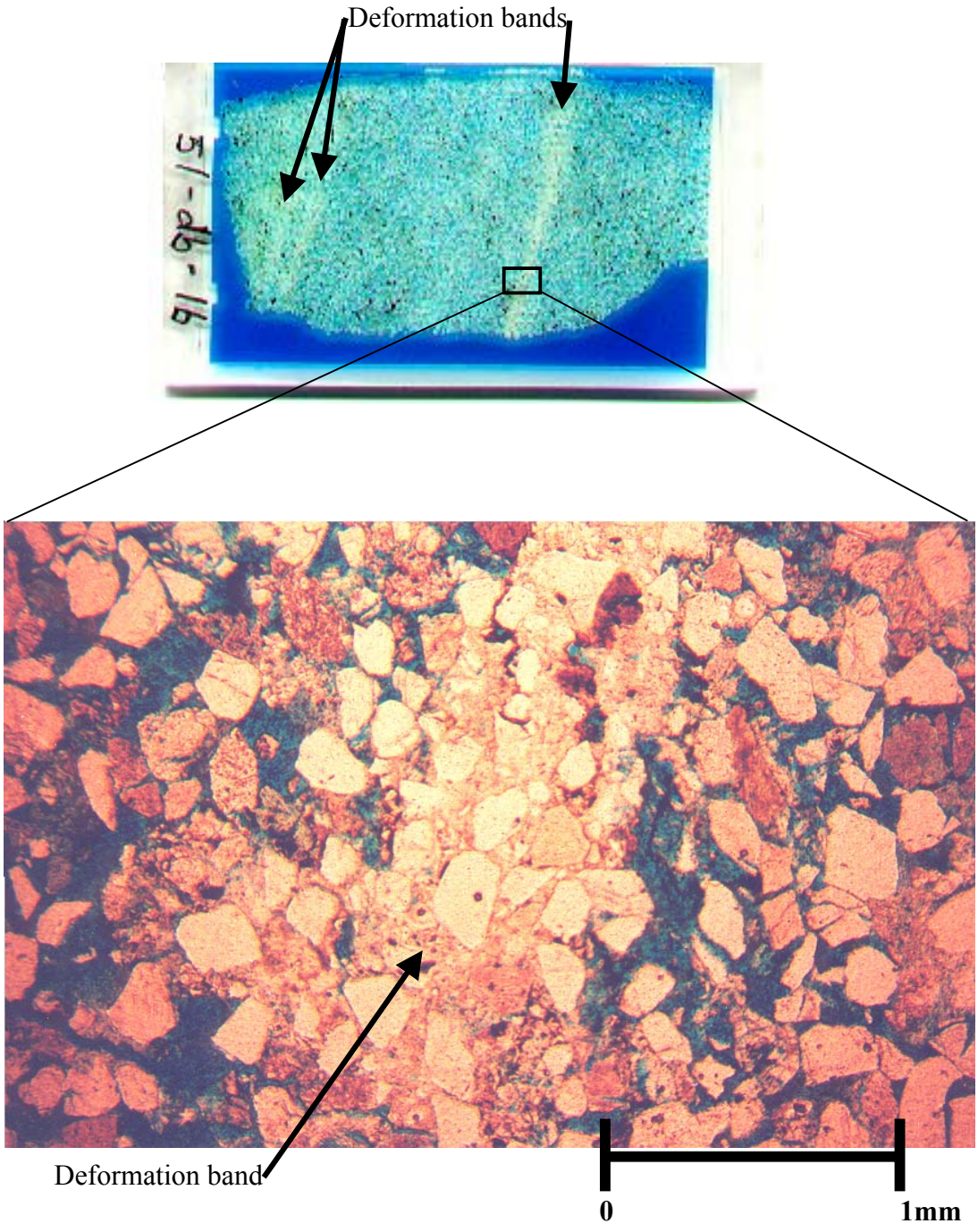

Figure 10: (A) Scanned image of a petrographic slide showing deformation bands within Unit 3 white beach sandstone. (B) Plain light photomicrograph of a deformation band within the petrographic slide shown in A. Sample was impregnated with blue epoxy to highlight porosity. Note the decreased porosity within the deformation band relative to the surrounding matrix.

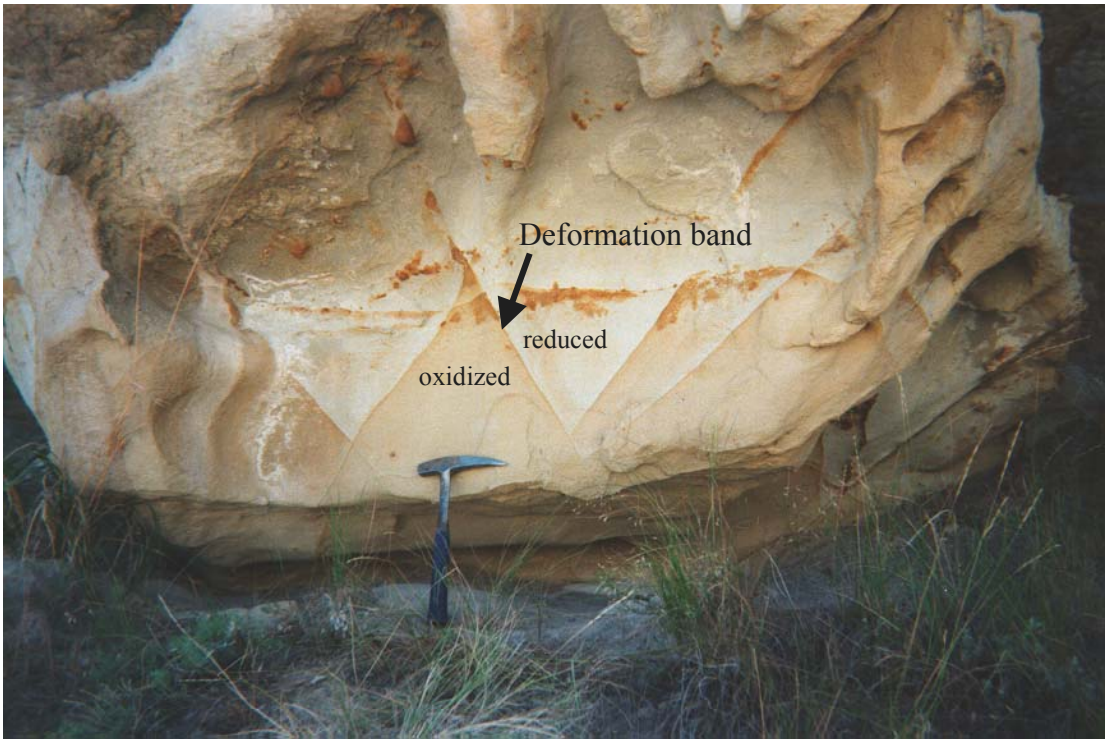

Figure 11: Conjugate deformation bands with a vertical bisector to the acute angle. Note reduced iron above the deformation bands and oxidized iron below.

2.4.2 Faulting

Faults at Teapot Dome show variable characteristics associated with differences in porosity and cementation of the rock units cut by the fault. Fault character changes radically where a given fault cuts both poorly cemented sandstone and well cemented sandstone. These changes reflect the differences in deformation behavior documented in previous sections. Faults within well cemented sandstones typically have damage zones characterized by high fracture density. The fractures associated with these faults typically strike parallel to the faults and dip normal to bedding. Where the same fault transects the high porosity, poorly cemented sandstones of the white beach facies (Unit 3) it is expressed as a zone of subparallel deformation bands.

2.4.3 Mineralization

Faults and associated fractures are variably cemented. Well cemented faults tend to stand out as erosion-resistant ridges or spurs; poorly cemented or uncemented faults, in contrast, weather into gullies. Cements observed at Teapot Dome are typically calcite, but pyrite is also locally present. Iron staining along fractures and up to 4 cm into the matrix parallel to fracture planes is observed locally. This indicates some fluid flow communication between the fracture and matrix. The degree of cementation of structures varies abruptly in space. In one area, a well cemented fault is located just 50 m from a highly weathered fault that is inferred to have little or no cement.

Fractures at thirty-eight sites around Teapot Dome were mineralized with either calcite or iron oxides. Iron oxide mineralization was evidenced by iron staining, both on the fracture surface and at some distance (1 - 4cm) into the matrix from the fracture. Sixteen of the sites were within Unit 1 sandstones, of which fractures at eleven sites were mineralized with calcite, fractures at two sites were mineralized with calcite and small amounts of pyrite, fractures at two other Unit 1 sites were iron stained, and fractures at the one site contained both iron staining and calcite mineralization. Calcite mineralized fractures within Unit 1 were generally associated with NE-SW oriented faults along the northeastern segment of the anticline. At eleven of the thirty-eight sites cleats within Unit 4 (carbonaceous shales) were mineralized with iron-oxide. Fractures within Unit 5 (fluvial sandstones) at four sites were mineralized. Fractures at two of these sites were mineralized with calcite, at one site with iron oxides and at the other site with gypsum. Fractures at two sites within Unit 3 sandstones were iron stained. Fractures at three sites within Unit 2 sandstones were mineralized, fractures at two of these sites were mineralized with calcite and fractures at the remaining site were mineralized with iron oxides. The two remaining sites were within the Steele Shale and the fractures were mineralized with calcite.

The majority of mineralized fractures were partially occluded. Fractures at four of the five sites generally sealed with calcite were within Unit 1 sandstones. Calcite filled fractures at the fifth site were within Unit 2 sandstones.

2.4.4 Subsurface Structures

The shallowest reservoirs at Teapot Dome are in the Shannon Formation. The sandstones within this formation were deposited as offshore bars along the western margin of the Cretaceous Western Interior Seaway (Tillman and Martinsen, 1984; Tillman, 1985). The Shannon Formation contains bar margin, inter bar and bioturbated shelf sandstones. The Shannon Formation has been cored extensively at Teapot Dome, and is exposed in outcrop at the Salt Creek anticline. About 300 ft of core from the Shannon Formation, in nine wells, at Teapot Dome was examined for fractures. This formation is one of the main producing intervals at Teapot, and is located at depths between 250-650 ft (76-198 m) subsurface. None of the cores are oriented.

The Shannon Formation at Teapot consists primarily of heavily bioturbated clayey sandstone. Bioturbation has reworked and destroyed most primary sedimentary structures in this sandstone, and, for this reason, only a few thin (two inches to two feet thick) clean sandstones are present. The sandstones commonly become glauconitic near the top of the reservoirs. Intervals of shale and silty shale separate the sandy reservoir units.

Two types of fractures occur in the Shannon Formation. The first type consists of vertical extension fractures that are typically limited to the thin, clean sandstones, terminating at bedding contacts with the clayey bioturbated sandstones (Figure 12). The second type of fracture is really a small fault or series of faults that occur within the muddier sandstones and in the shale intervals between reservoir beds (Figure 13).

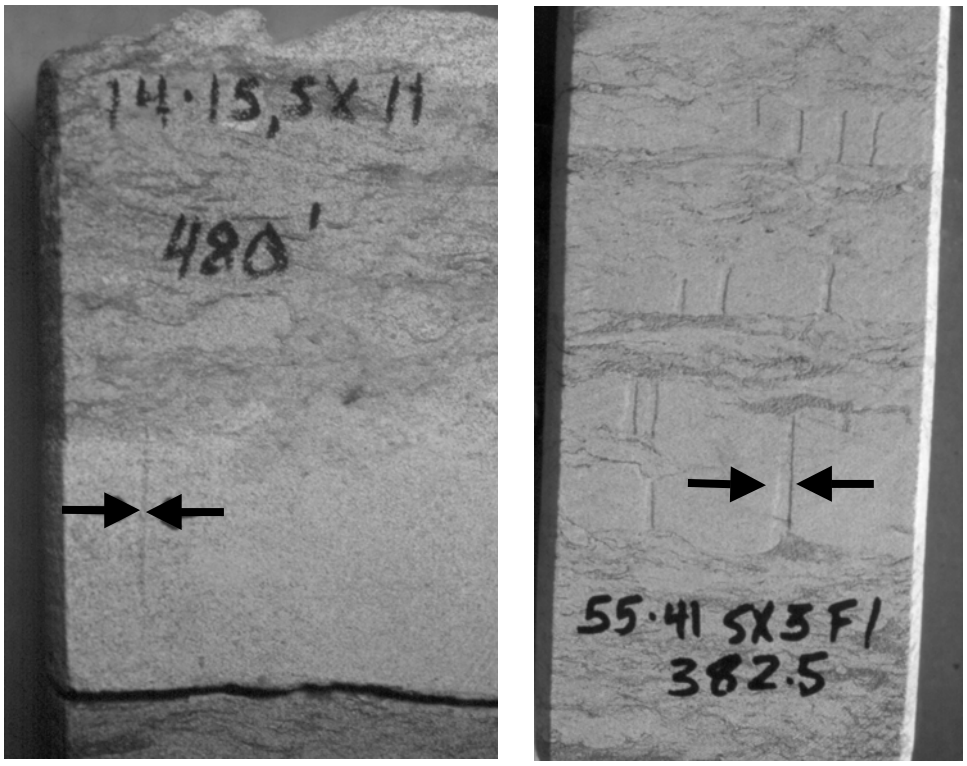

A B

Figure 12: Slabbed, four-inch diameter Shannon Sandstone core. A) Core from 480' depth in well 1415SX11. Upper half of core is representative of the bioturbated facies. The lower half is representative of a cleaner sandstone with a natural fracture located between the arrows. B) Clean sandstones interbedded with bioturbated sandstones at 382.5' depth in well 5541SX3 F1. The light colored, calcite cemented natural fractures are highlighted by pencil marks along the right side of the fracture. The fractures are limited to the cleaner sandstones.

2.4.4.1 Fractures

Nine unmineralized vertical fractures, and six vertical calcite-mineralized fractures were observed in the Shannon cores. These fractures range from one inch to slightly over one foot tall along the axis of the core. The unmineralized fractures tend to be only roughly planar whereas the mineralized fractures are closer to vertical and more planar. The calcite-mineralized fractures have significant remnant porosity (estimated at up to 20% of the mineralized fracture apertures, which are up to 2 mm wide in the taller fractures). In addition to the six isolated calcite-mineralized fractures, two zones of swarms of calcite-mineralized fractures were noted in two of the thicker sandstones. One, a 3.5 ft (1.06 m) thick bed of cleaner sandstone in the 22S14 well (614-617.5 ft; 187-188 m depth), contains a series of short irregular vertical fractures. All of these fractures have parallel strikes, and the largest is 1.2 ft (0.36 m) tall.

Vertical fractures are most common in the cleaner Shannon sandstones (Figure 12). Unfortunately, since clean sandstones are rare, these fractures are not present throughout the Shannon reservoirs at Teapot. The clayey, bioturbated, Shannon sandstones are generally not susceptible to fracturing, as indicated by hammer-impact points on the core where the attempt

was made to shorten pieces for boxing. In these cases the core absorbed the hammer blow rather than cracking. However, the fact that numerous vertical fractures were intersected at all indicates that fractures are probably common in those intervals where the Shannon is susceptible to fracturing.

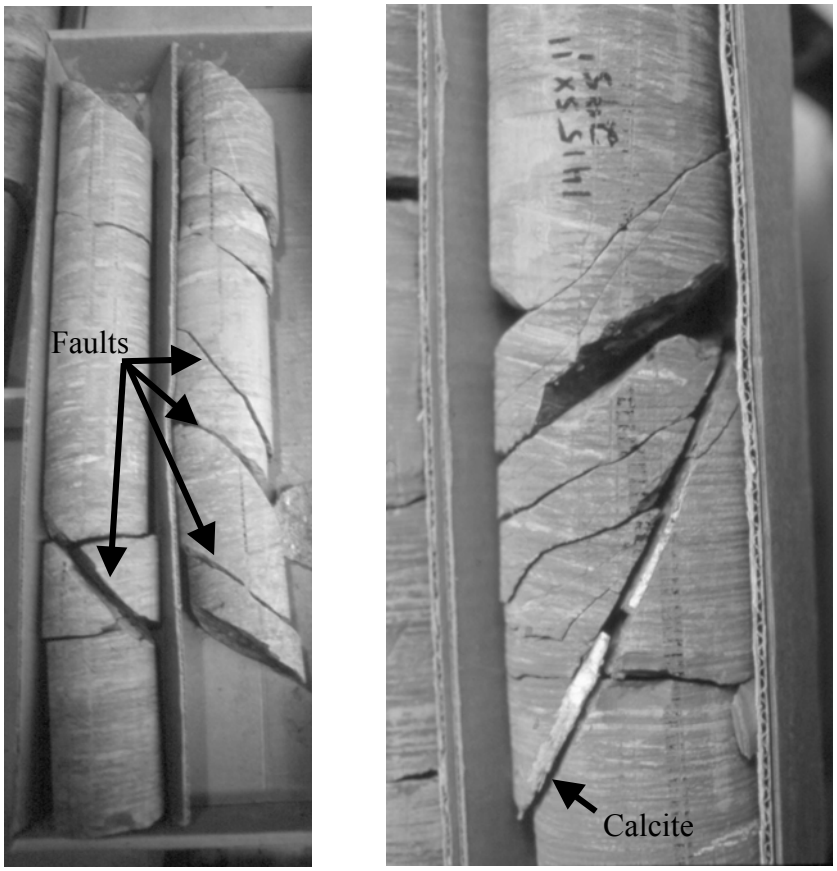

Figure 13: Faults with normal displacement observed in four-inch diameter core from well 1415 SX11. A) Series of subparallel faults at a depth of 237'. Four of the fault planes are highlighted with arrows. B) Close-up view of a fault at a depth of 295'. White color along fault plane is calcite mineralization.

2.4.4.2 Induced Fractures

No coring-induced petal fractures were observed in these cores, consistent with the implied resistance to fracturing of the Shannon sandstones. For this reason there is no way to tell the relative orientation between the vertical fractures and the present-day, maximum horizontal compressive stress in these strata. Numerous irregular centerline fractures occur in these cores, commonly in the shaley intervals but also in the clayey sandstones.

2.4.4.3 Faults

The cored faults may be mineralized with calcite or they may be unmineralized (Figure 13). They typically have surface lineations that indicate dip-slip or slightly oblique dip-slip

displacement, although whether this is normal or reverse displacement is usually difficult to tell. Normal displacement is more likely since most of the faults are relatively high angle (dipping 45^{o}-75^{o}). Locally up to 6 sub-parallel fault planes occur within short (eight inch) core intervals. Mineralization, where present, consists of layers of calcite up to 2 mm thick (Figure 13) and is commonly patchy where the fault plane is irregular.

2.5 Discussion

2.5.1 Fracture spacing vs. bed thickness

Exposures of the Mesaverde Formation at Teapot Dome provide an excellent opportunity to study fracture and fault variability related to lithology. One of the first assumptions relating lithology to fractures is that fracture spacing is directly proportional to bed thickness (McQuillan, 1973; Narr and Suppe, 1991; Gross, 1993; Ji and Saruwatari, 1998; Bai and Pollard, 2000). Data from Teapot Dome indicates that this relationship, although broadly proportional under certain conditions, is not 1:1. In fact, cleat spacing in Unit 4 carbonaceous shales and coals consistently remains below 0.5m no matter what the bed thickness. The data also show that there is an inverse relationship between cleat spacing and bed thickness within this unit (Figure 7). Price (1966), as noted earlier, uses Young's modulus to explain the differences between fracture spacing in sandstones and cleat spacing in coals; it appears that mechanical controls dominate over bed thickness in these lithologies. The difference between cleat and fracture strike in carbonaceous shales and sandstones respectively, may also be due to differences in mechanical properties. A possible explanation regarding the inverse spacing relationship from a mechanical standpoint is that thinner coals may be less brittle than thicker coals, therefore cleats are more widely spaced in thin units relative to thicker units. However, it is equally possible that there is some difference between measurable bed thickness and effective (mechanical) bed thickness, perhaps due to horizontal layering within the carbonaceous shale beds.

As previously discussed, Bogdanov (1947) mathematically described a relationship where spacing (S) varied as a function of bed thickness (B) and some constant (K). The amount of variation from an idealized 1:1 fracture spacing to bed thickness ratio can provide some visualization as to how the constant (K) varies with lithology and mechanical controls. Fracture spacing in Unit 2 sandstones is poorly correlated with bed thickness (Figures 5 and 7). These sandstone beds are generally interbedded with other sandstone beds. In contrast Unit 1 and 5 sandstones, interbedded with marine shale and carbonaceous shale respectively, exhibit the strongest correlation between fracture spacing and bed thickness. Therefore, sandstones within these units have distinctly different boundary layers than Unit 2 sandstones and these bounding layers may contribute significantly to the fracture spacing to bed thickness ratio. Unit 5 is the nearest to 1:1 fracture spacing to bed thickness ratio (when combining all fracture sets). The Unit 5 sandstones are laterally discontinuous while the other sandstone units are laterally continuous suggesting that there is some lateral mechanical influence on fracturing. The spacing relationships between oldest throughgoing fractures, younger throughgoing fractures and cross fractures also indicates some lateral mechanical influence on fracture spacing. Specifically the younger throughgoing and cross fracture sets have spacings larger than the oldest throughgoing fracture set, suggesting the older fractures are planes of discontinuity that influence fracture spacing in younger fracture sets.

No data were collected concerning the paleoflow direction within any of the units. Therefore, a word of caution is added that some of the variability observed in fracture spacing and fracture orientation may be due to mechanical anisotropy inherent to beds with a grain fabric related to deposition (Committee on Fracture Characterization and Fluid Flow; 1996). Depositional trends such as thickening and thinning of units may also influence local fracture spacing.

2.5.2 Outcrop to subsurface comparison

Thrusting at Teapot Dome, as evidenced in 2-D seismic reflection data, terminates within the lower Paleozoic section. Since the fold does not appreciatively "tighten" within the Cretaceous section, extrapolation of fracture orientations observed within the Mesaverde Formation to shallow reservoir sandstones should be possible. Vertical fractures are common within clean Shannon Sandstone lithologies that were susceptible to fractures. Therefore, the Shannon Sandstone fracture system should be similar to that within the Mesaverde Formation. The Mesaverde outcrop fracture study should also be applicable to the Cretaceous Wall Creek (Frontier) reservoirs at Teapot Dome. The Wall Creek strata were deposited by prograding fluvial systems similar to those within the Mesaverde Formation. Therefore, these rocks should have similar fracture patterns given similar lithologic and structural controls.

Allowances may need to be made for changes in the Teapot Dome structure with increasing depth. This may be particularly true for deep reservoir units such as the Tensleep Sandstone. In these cases fracture orientations may vary from those observed in the outcrop.

2.5.3 Impact of structures on fluid flow

From a production standpoint, fracture permeability is highly dependent upon the following variables: 1) trace length, 2) aperture width, 3) interconnectivity of the fracture system, and 4) the number of fractures intersecting the well bore. Core data provides information on aperture width and number of fractures intersecting the well bore. However, due to the small size of the core, information with regard to trace length and fracture interconnectivity can be limited. Outcrop fracture studies can help fill in information for the last two items.

Fractures, in a sense, work like a plumbing system for the reservoir. The longer and more interconnected the drainage system the better the recovery. Fractures with extensive trace lengths have the potential of more effectively draining a reservoir than shorter fractures. The increased fracture surface area associated with increased trace length allows for increased fluid flow communication between the rock matrix and the fracture. Therefore, a well that intersects a fracture set with extensive trace lengths has the potential of draining a significantly larger area than a well that intersects no fractures or fractures with a limited trace length.

In outcrops at Teapot Dome, depending upon the lithology of the faulted rock unit, a single fault can be expressed as either a zone of deformation bands (partial barriers to flow) or a fault with a primary slip plane and an associated fracture zone (a possible fluid pathway). Unit 3 sandstones, which contain deformation bands, vary in thickness across the anticline, and are

locally absent along the western limb. How this change in thickness influences regional fluid flow is undetermined. However, both in units with deformation-band faults and in those with fracture-based faults, maximum permeability would be parallel to fault strike. In the former, fluid flow would be largely confined to the matrix. In the latter, fluid flow would occur preferentially along fractures as long as they remained unmineralized. Therefore, in low permeability rocks, fractures will be the primary pathways for fluid flow. In contrast, in the high porosity sandstones that host deformation bands, the matrix will provide the main pathway for fluid flow. Relatively well cemented, low porosity sandstones typically do not make a better reservoir than poorly cemented, high porosity sandstones. However, it is apparent from this study that natural fracturing will help increase production in more brittle sandstones while deformation bands may hinder production within high porosity sandstones.

As discussed previously, Thom and Spieker (1931), through work at Teapot Dome, recognized that mineralized faults and fractures may inhibit fluid flow and that open fractures could allow for increased fluid flow. However, they assumed that fractures would penetrate both sandstones and shales and that reservoir pressures would equalize. Because pressures within different reservoirs were not equal, the authors concluded that fractures did not significantly influence fluid flow. However, the current study shows that sandstones and shales do not fracture in similar ways. In fact, fractures within sandstone beds often terminate at sandstone/shale contacts. Core data from the Shannon Sandstone indicate fracture enhancement of vertical reservoir permeability is limited because fractures are limited in vertical extent to the thin cleaner sandstones. Horizontal, fracture-enhanced permeability within these sandstones should still be good. These relationships suggest that shales can create an effective seal between production zones and that pressures need not be similar across this fractured reservoir.

2.6 Conclusions

Fractures, deformation bands and faults within the Cretaceous Mesaverde Formation at Teapot Dome display patterns that vary with lithology in the following ways: 1) Most fractures in sandstone units terminate at contacts with shale layers. 2) Carbonaceous shales (Unit 4) have cleat spacing densities comparable to or greater than those within sandstones. However, unlike fractures in sandstone, cleat spacing has a unique inverse correlation to bed thickness. 3) In beds of similar thickness and close proximity cleat strike is oblique to fracture strike by up to 20^{o}. 4) Fracture density increases with increased cementation in sandstones. 5) Sandstones interbedded with marine shales or carbonaceous shales have a fracture spacing to bed thickness ratio that is closer to 1:1 than sandstones interbedded with other sandstones. Within this context fluvial sandstones with lenticular geometries interbedded with carbonaceous shales have a fracture spacing to bed thickness relationship that is closest to 1:1 of all the units. 6) The poorly cemented, high porosity sandstones of Unit 3 contain deformation bands rather than fractures. 7) Deformation bands have significantly lower porosities relative to the matrix due to crushing of grains within the deformation band. 8) Normal faults within well cemented sandstones are generally expressed as fracture zones, whereas faults within poorly cemented sandstones are diffuse zones of subparallel deformation bands. 9) Thinner sandstones (< 1m) interbedded within shale may be more likely to be mineralized than thicker sandstone packages.

In the absence of significant subsurface data and because factors such as porosity,

cementation and lithology can change with depth, a data set built from observations of outcropping strata that are lithologically analogous to subsurface reservoir rocks may allow a first-order approximation of what features (i.e. fractures, faults, and deformation bands) are present within the subsurface, their spacing and how they may influence permeability and fluid flow.

3.0 STRUCTURAL CONTROLS

3.1 Introduction

Rocks, in general, exhibit increased fracture density with increased deformation (Nelson, 1985). One method of predicting fracture density relative to structural position is the radius-of-curvature or rate-of-change approach (Murray, 1968). The major assumption of this approach is that the greatest density of flexure-related fracturing will occur where the rate of change of dip or curvature of beds is at a maximum (Nelson, 1985), such as in a fold hinge. Murray (1968) noted that the relationships between bed thickness, structural curvature and fracture porosity and permeability can be effective in evaluating geologic structures as hydrocarbon reservoirs.

Faults exert structural controls on fracturing. Fault zones in rock generally consist of a fault core and a damage zone, which have permeabilities distinctly different from the unfractured strata (e.g., Caine et al., 1996). The damage zone may include small subsidiary faults, fractures and veins. These structures can vary in character and density along the length of a fault due to variations in lithology and mineralization (see Section 2: Lithologic Controls). Displacement also varies along a single fault from a maximum at the center to a minimum at the fault tips (Nicol et al., 1996). Therefore, the density of secondary fault structures may be greatest near the center of the fault and decrease toward the fault tips, along both strike and dip. Secondary fault structures such as fractures within a damage zone can create areas of increased transmissivity. This can result in preferential fault-parallel fluid flow (Haneberg, 1995). Huntoon and Lundy (1979) describe a field example near Laramie, Wyoming wherein transmissivity is increased within rock units of the Casper aquifer system adjacent to fault zones and monoclines. The transmissivities of the fracture zones were found to be approximately 100 times greater than transmissivities of unfractured areas. In other situations, decreased porosity within a fault zone could produce a capillary seal given two liquids such as water and oil (e.g., Antonellini and Aydin, 1995; Sigda et al., 1999). Compartmentalization of a petroleum reservoir could occur should the capillary seal prevent cross-fault flow of the nonwetting phase (e.g., oil in a water-wet reservoir; Antonellini and Aydin, 1994).

The permeability of fractures can also be influenced by changes in pore fluid pressure. The effective normal stress can be increased by a decrease in pore fluid pressure causing fractures at a high angle to the maximum principal stress to close (Lorenz et al., 1996; Committee on Fracture Characterization and Fluid Flow, 1997). Therefore, as fluids are removed during production of a fractured reservoir, in situ pore pressure may drop, decreasing the aperture widths of critically oriented fractures, which in turn decreases effective permeability and production. Substantial reduction in reservoir pressures at Teapot Dome, for example, is suspected from early production reports (Trexel, 1930; Curry, 1977; Doll et al., 1995).

A systematic study of natural fracture patterns within the outcropping Mesaverde Formation at Teapot Dome was undertaken, in part, to understand variations in fracture characteristics, such as spacing and orientation, with structural position on a doubly plunging anticline. Field observations indicate that extension fractures and normal oblique faults, roughly perpendicular to the fold hinge, are contemporaneous with hinge-parallel faults and fractures. A third set of fractures with a strike oblique to the fold are interpreted to predate folding.

An important first step in understanding the nature of permeability anisotropy is developing a conceptual model of the orientations and distribution of structures that influence flow, such as fractures and faults. Various models have been proposed to explain the variation in orientation, location and spacing of fractures in basement-cored anticlines (DeSitter, 1956; Stearns and Friedman, 1972; Pollard and Aydin, 1988; Engelder, 1997; Lorenz, 1997). Many of these conceptual models were developed from field observations at petroleum reservoirs and outcrops. These models are then applied to similar reservoirs for predictive purposes. This use of analogous reservoirs for prediction of permeability anisotropy and localized areas of hydrocarbon accumulation is quite common within the petroleum industry (Stearns and Friedman, 1972; Nelson, 1985; Pollard and Aydin, 1988). The fracture and fault data and interpretations from Teapot Dome are used with previous studies to develop a 3-D conceptual model of fractures associated with basement-cored anticlines. A qualitative assessment of the 3-D model suggests that the direction of maximum permeability can be either parallel or perpendicular to the fold hinge depending on the primary fracture pattern within a specific area of the fold.

Another purpose of this research was to evaluate the utility of existing conceptual models by comparing the orientation and distribution of predicted structures with those observed at Teapot Dome, Wyoming. Similarities exist between the patterns observed at Teapot Dome and those described or postulated by DeSitter (1956), Murray (1967), Simon et al. (1988), Garrett and Lorenz (1990), Engelder et al. (1997), Hennings et al. (1998), Unruh and Twiss (1998) and Hennings et al. (2000). However, the orientations of two primary fracture sets predicted by one of the most widely used models (i.e., Stearns and Friedman, 1972) are significantly different from those observed at Teapot Dome. The importance of using a model most analogous to a specific petroleum reservoir for analysis and prediction of permeability anisotropy cannot be over-emphasized. In general, the most analogous reservoirs and models would be those with mechanically similar stratigraphic units, which formed under a similar tectonic regime.

3.2 Fracture-Fold Relationships

Several authors have described preferred fracture orientations associated with folding (DeSitter, 1956; Stearns and Friedman, 1972; Simon et al., 1988; Garrett and Lorenz, 1990; Cooper, 1992; Berry et al., 1996; Engelder et al., 1997; Hennings et al., 1998; Hennings et al., 2000). Observations from these studies can be subdivided into two main categories, those related to thin-skinned thrusts and those related to basement-cored thrusts.

3.2.1 Folds associated with thin-skinned thrusts

Stearns and Friedman (1972) described five fracture sets associated with folds, only two of which are stated as being sufficiently common to be incorporated into their generalized fracture model. These fracture patterns were documented at the Teton anticlines in northwestern Montana (Stearns, 1964; Stearns, 1967, Friedman and Stearns, 1971; Sinclair, 1980). The Teton anticlines are a pair of Laramide-age structures, and are part of a thrust sheet within the sedimentary section rather than a basement-cored anticline. The larger, western most anticline is hereafter referred to as Teton anticline. The two main fracture sets each consist of extension fractures and conjugate shear fractures (Figure 14). The sets locally occur together within the same beds. Both sets are interpreted to record an intermediate principal stress (σ_2) normal to bedding and maximum (σ_1) and minimum principal (σ_3) stresses within the bedding plane. The orientations of maximum and minimum principal stresses were inferred to be different for each fracture set (Figure 1). The geometry of these patterns suggests that they accommodated shortening both parallel and perpendicular to the fold hinge. Stearns and Friedman (1972) suggested that these fracture sets resulted from folding because of their consistent orientations relative to bedding and the anticlinal structure. A third set of fractures, described by Stearns (1964), accommodated extension due to bending of the formations across the anticline.

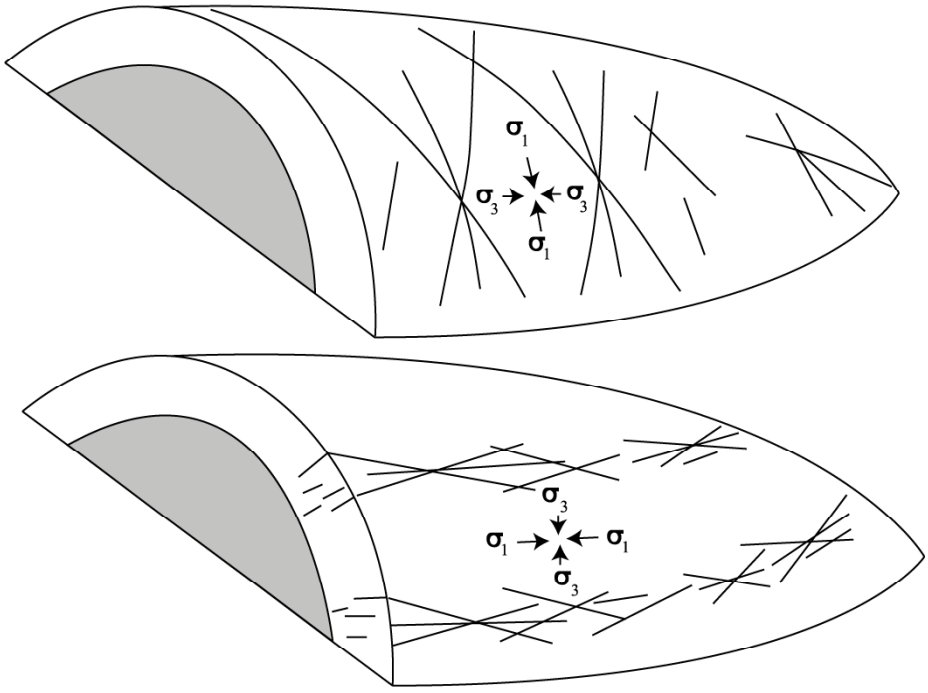

Figure 14: Stearns and Friedman (1972) model of fractures associated with folding. In both fracture sets the intermediate principal stress (σ_2) is inferred to be normal to bedding and the maximum (σ_1) and minimum (σ_3) principal stresses therefore lie within the bedding plane. The inferred directions of maximum and minimum principal stresses are different for each fracture set.

Cooper (1992) used core analysis along with Formation Microscanner and Array Sonic logs to analyze subsurface fractures associated with a fault-bend fold and a fault-propagation fold in the foothills of the Canadian Rocky Mountains. Extension fractures parallel and perpendicular to the fold hinge were recorded as were conjugate shear fractures, all of which correspond to the two dominant fracture sets described by Stearns and Friedman (1972).

Berry et al. (1996) also record extension fractures parallel and perpendicular to the fold hinge near the culmination of the Palm Valley anticline within the Amadeus Basin of central Australia. Conjugate fractures that correspond to the extension fractures were also observed. It should be noted that the dominant fracture sets change orientation with respect to the fold, i.e. the fracture set parallel to the fold hinge at the culmination of the fold is perpendicular to the fold hinge within the plunging nose of the fold (Berry et al., 1996). Essentially the fractures are oriented relative to bedding strike and not fold orientation within this particular study area and model.

3.2.2 Folds associated with strata overlying deep-seated thrusts

Dominant features associated with basement-cored thrusts include hinge-parallel and hinge-perpendicular faults and fractures. The following examples primarily describe these features and/or describe how they may be related to the folding process. DeSitter (1956) described normal faults parallel to a given hinge that were attributed to tension within the upper arc of an anticline and were observed at Kettleman Hills, California; Quitman Oilfield, Texas; Sand Draw Oilfield, Wyoming; and La Paz Oilfield, Venezuela. Normal faults roughly perpendicular to the axes of folds were attributed to tension resulting from the three-dimensional nature of an uplift (DeSitter, 1956). These faults exhibit maximum displacements near the apex of a given anticline. Further, the displacements on hinge-perpendicular faults decrease toward the limbs of the fold. Both DeSitter (1956) and Engelder et al. (1997) discussed these types of faults using examples from Elk Basin oilfield in Wyoming. Elk Basin anticline is a basement-cored, doubly plunging, breached anticline in the Big Horn Basin with dips on the forelimb in excess of 30^{o} and up to 23^{o} on the backlimb. The anticline strikes roughly NNW and is cut by a number of normal oblique, NE-striking, hinge-perpendicular faults. Fractures striking roughly parallel to the fold hinge are found throughout the fold, but vary more in orientation along the forelimb, perhaps due to local faulting (Engelder et al., 1997). Fractures striking roughly perpendicular to the fold hinge were found in 12% of measured outcrops and are composed of two basic types: fractures with trace lengths extending several meters and fractures that are confined to the area between hinge-parallel fractures. Thus these later hinge-perpendicular fractures terminate at intersections with hinge-parallel fractures.

Similar joint sets oriented parallel and perpendicular to the hinge of the Grand Hogback Monocline in Colorado were observed (Murray, 1967). The development of these fractures was inferred to be related to local uplift and rotation of bedding rather than regional shortening. Penecontemporaneous development of the two joint sets was suggested by the lack of consistent abutting relationships to indicate which set is older. However, Garrett and Lorenz (1990) did recognize an older fracture set along the same Grand Hogback Monocline. They interpreted this set, composed of throughgoing regional fractures, to be associated with shortening prior to folding. Two other fracture sets - those recognized by Murray (1967) - were associated with

folding along the Hogback.

Hennings et al. (1998; 2000) described three joint sets within Frontier Formation sandstones at Oil Mountain, approximately 30 miles west of Casper, Wyoming. Oil Mountain is a NW-striking, doubly plunging, breached anticline. Oil Mountain is unique in this deep-seated thrust category as it is interpreted to have thrust faults in the Mesozoic section that are related deeper basement thrusts. A NW-striking fracture set parallels the fold hinge at Oil Mountain but is interpreted as a pre-existing regional set due to its presence in Frontier Formation pavements away from the fold. A NE-striking set is roughly perpendicular to the NW-striking set and is attributed to the folding process. The third set is NNW-NNE striking and is oblique to the fold hinge and the other two joint sets. A substantial increase in fracture density was observed within the southern plunging region of the anticline.

Because these anticlines and monoclines are cored by reverse faults it is worth considering strain around a blind thrust. Unruh and Twiss (1998) used coseismic displacements measured after the Northridge earthquake of 1994 (which resulted from movement along a blind thrust fault) to determine the orientations of the principal strain-rate axes for a blind thrust. Horizontal shortening (d_3) is perpendicular to the fold hinge, maximum lengthening (d_1) is horizontal and parallel to the fold hinge and d_2 is vertical.

Using pseudo-three-dimensional modeling and curvature analysis, Fischer and Wilkerson (2000) described fracture patterns in sedimentary units, modeled as elastically deformed plates, during the evolution of a basement-involved thrust fault. They described joints oblique to the fold hinge as being related to the formation of a fold. These oblique fractures can form early in the folding process. Their work indicates the timing of fracture initiation relative to fold development is a control on fracture orientation. They also noted that fracture orientations may vary with stratigraphic and structural position.

3.3 Structural Analysis of Teapot Dome

Fractures, faults, and deformation bands were studied in five lithologically distinct stratigraphic units within the Mesaverde Formation at Teapot Dome. These units are (from oldest to youngest): a shallow marine interbedded sandstone/shale, a foreshore/beach sandstone, a white beach sandstone, a non-marine carbonaceous shale, and a unit composed of fluvial sandstones within the carbonaceous shale unit. Detailed discussion of these units and of lithologic controls on fracturing is provided in Section 2: Lithologic Controls.

3.3.1 Distribution of faults and fractures with respect to the fold

3.3.1.1 Faults

Two dominant sets of faults are observed in outcrops of the Mesaverde Formation at Teapot Dome. The first set consists of NE-striking normal oblique faults shown on Figure 14. These faults are common along the eastern limb and most terminate before intersecting the western limb; displacements therefore decrease to the SW. A normal component of displacement is recorded by stratigraphic separation whereas the strike-slip component is

inferred from slickenlines on three fault surfaces with rakes of 20^{o}–35^{o}. Sense of slip for these three faults is oblique right lateral. These faults are generally perpendicular to the fold hinge, even where it bends, and are characterized by vertical separations that vary across the fold. The largest separations, up to 40 m, are observed on the eastern limb. The few hinge-perpendicular faults observed in surface exposures on the western limb exhibit vertical separations that range between 0.5 and 1 m. Although continuous exposure is not available around the dome, these hinge-perpendicular faults appear to be densest near the culmination of the fold (Figure 15).

Two faults near the apex of the anticline, observed in 2-D seismic reflection profiles (from the Rocky Mountain Oilfield Testing Center), can be projected into valleys along the western limb. There is little to no surface exposure of these faults. Individual segments of the western limb, separated by these valleys, display different bedding and fracture orientations (Figure 16); in each segment the strike of one primary fracture set roughly parallels the strike of bedding. These valleys are therefore interpreted as faults. Valley trends indicate that the faults belong to the NE-striking fault set.

There are two possible interpretations for the along strike orientation of NE-striking faults across the anticline. One interpretation is that the faults remain relatively parallel with only a few faults having lateral extents long enough to intersect the western limb (Figure 15). This interpretation is graphically illustrated in the figures for this report. This interpretation is based on interpolating surface measurements with the available subsurface data (2-D seismic and reservoir maps). A second plausible interpretation suggests that the faults along the eastern limb coalesce along strike to the west and form the valley faults in the western limb.

The second set consists of normal faults that strike subparallel to the fold hinge and are observed primarily along the southern arc of the anticline where curvature is at a maximum (Figure 15). Normal motion on these faults is recorded by stratigraphic separation.

Deformation bands are observed primarily within poorly-cemented sandstones. Lithologic controls on deformation band formation are discussed in Section 2.0. They commonly occur as conjugate pairs near the southern and southwestern margins of the anticline and as non-conjugate faults in other areas. The conjugate pairs are oriented such that there is a vertical bisector to the acute angle between a given pair. These small-displacement faults strike parallel to each of the three primary fracture orientations recorded at Teapot Dome. Normal separation associated with deformation bands ranges from indiscernible to approximately 20cm. The larger separations are associated with multiple (up to 20) inosculating deformation bands (inosculating deformation bands approach and diverge from each other but do not cross). Where displacement can be constrained, individual bands generally have 1-3 cm of normal separation. At four sites, deformation bands occur within the same bed as fractures. At a single site, deformation bands were nearly perpendicular to the throughgoing extension fracture set and terminate where they intersect the fracture set. Therefore, at this site the deformation bands post date fracture formation. The age of the deformation bands relative to fracture formation at the other sites is undetermined.

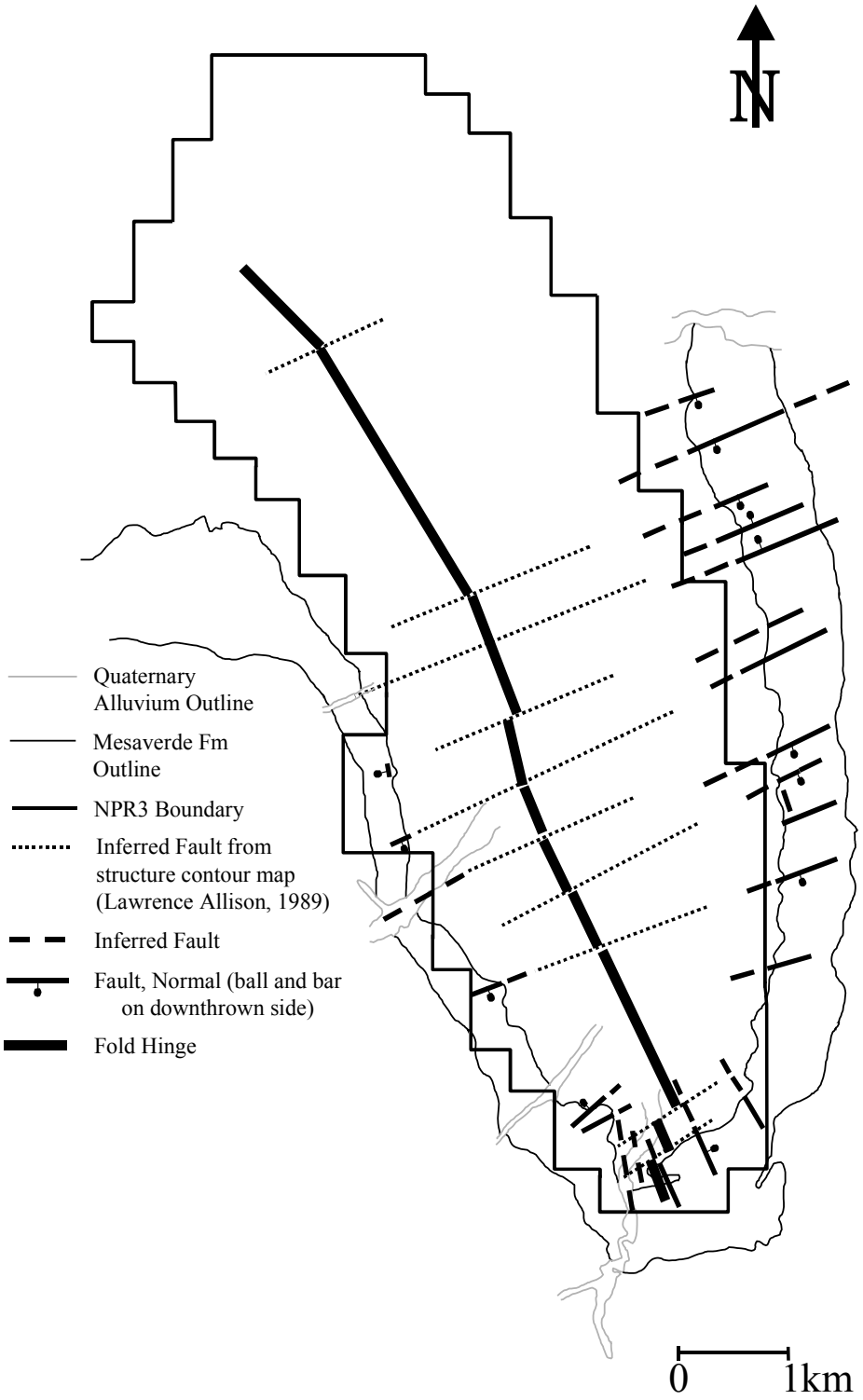

Figure 15: Primary faults observed at Teapot Dome, Wyoming. Because of poor exposure in the core of the dome, individual faults generally cannot be traced from the eastern to the western limb. Faults and fold hinge shown in the central portion of the anticline are inferred from a structure contour map on the top of the second Wall Creek Sandstone (Lawrence Allison, 1989) and field data.

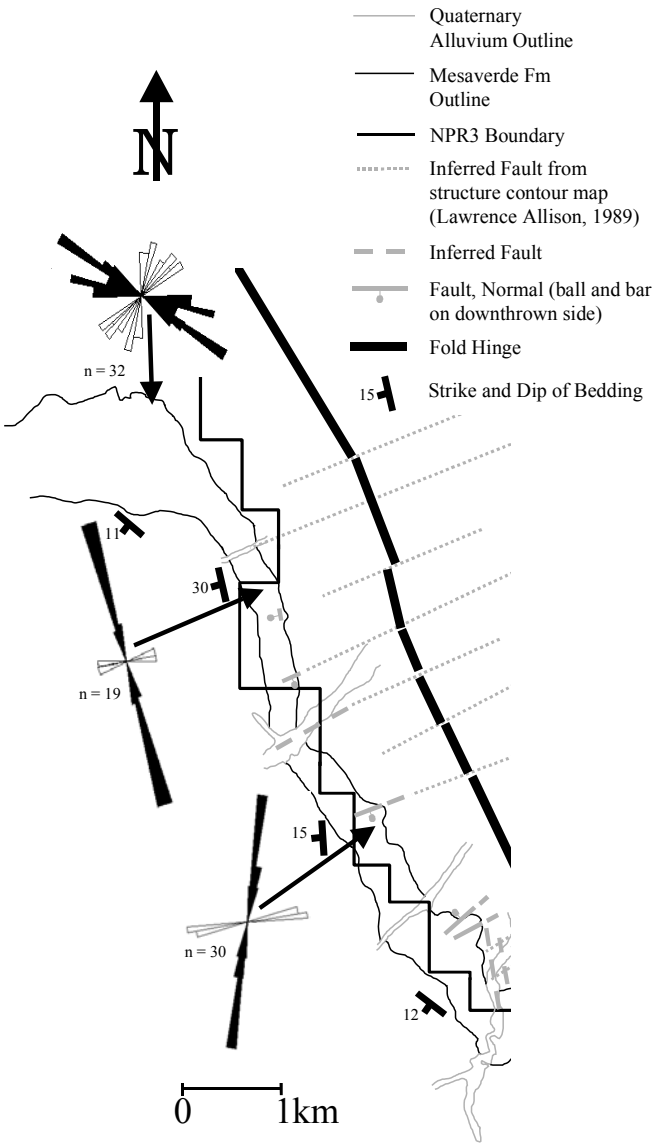

Figure 16: Map illustrating segmentation of the western limb. Fracture orientations of individual segments generally parallel bedding strike. Red sections of the rose diagrams illustrate the orientation of the throughgoing fracture sets.

3.3.1.2 Fractures

Three throughgoing fracture sets were documented at Teapot Dome (Figure 17). One fracture set includes fractures oblique to the fold hinge. Most of these strike roughly NW to WNW; a small number are roughly perpendicular to these, and thus strike NNE. A second set is subparallel to the fold hinge. The third fracture set is roughly perpendicular to the fold hinge. Forty-four percent of the documented fractures are parallel to the fold hinge, 32% are perpendicular to the fold hinge and 24% are oblique to the fold hinge.

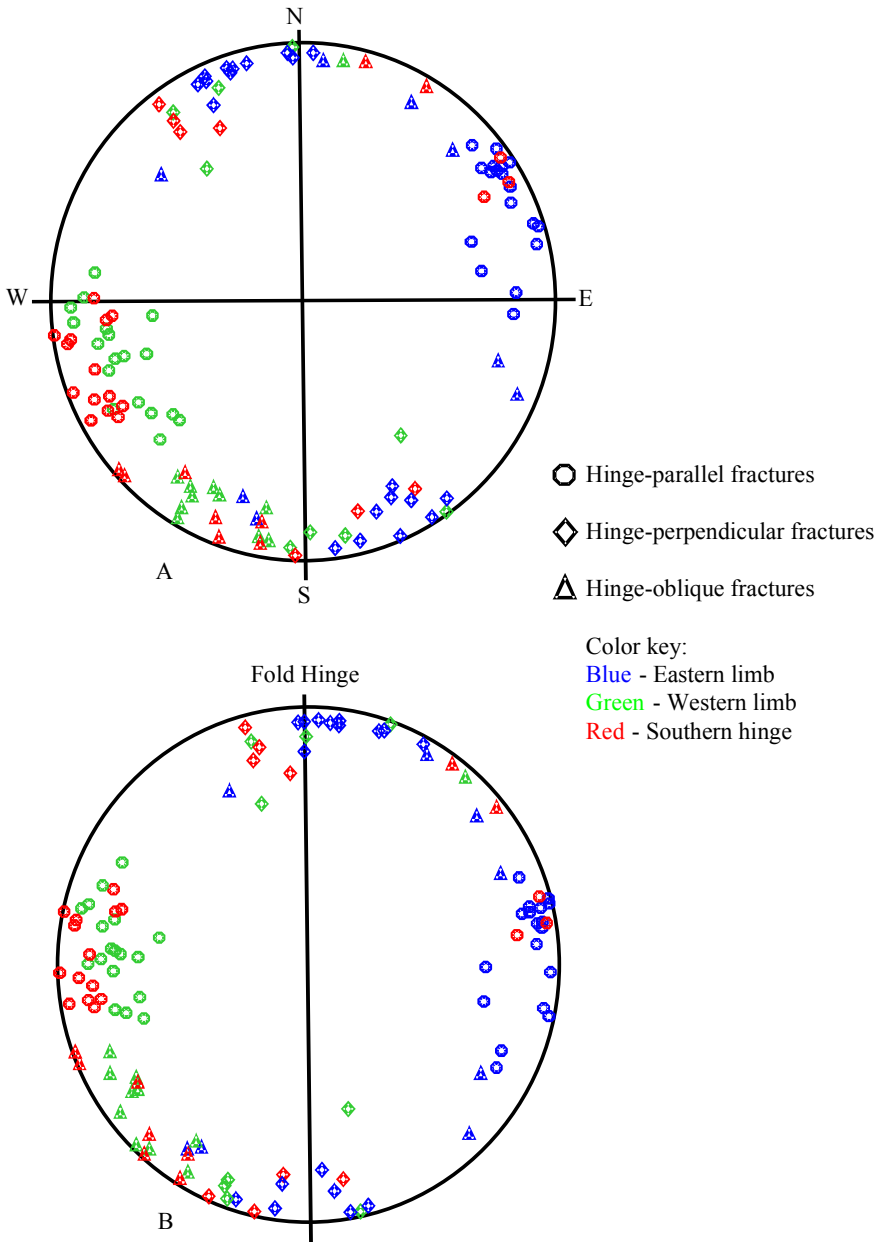

Figure 17: (A) Lower hemisphere equal area net plot of poles to 129 representative throughgoing fractures from 87 locations around Teapot Dome. (B) The same data set used in A, normalized to the fold hinge (data rotated so that fold hinge has orientation shown). Fractures are considered hinge-parallel if they strike ± 20° from the hinge; hinge-perpendicular fractures strike 90° ± 20° from the hinge.

The set of fractures which strikes oblique to the fold hinge is found at 28 sites throughout the fold and is equally distributed among the various lithologic units of the Mesaverde Formation (Figure 18). Three additional sites record deformation bands with the same general strike as the fracture set. At almost all sites this is the oldest set of fractures or deformation bands relative to the other throughgoing fracture sets as determined by abutting relationships. At only one site is

the oblique set younger than one of the other two fracture sets. At another site, the oblique fracture set is the only fracture set recorded. There are two oblique fracture sets with an approximate 10° difference in strike at two locations. One of the sets at these locations is younger than the other. However, relative age between oblique fractures and hinge parallel and/or hinge-perpendicular fractures could not be determined, because the later two fracture sets are not present at either of these two sites.

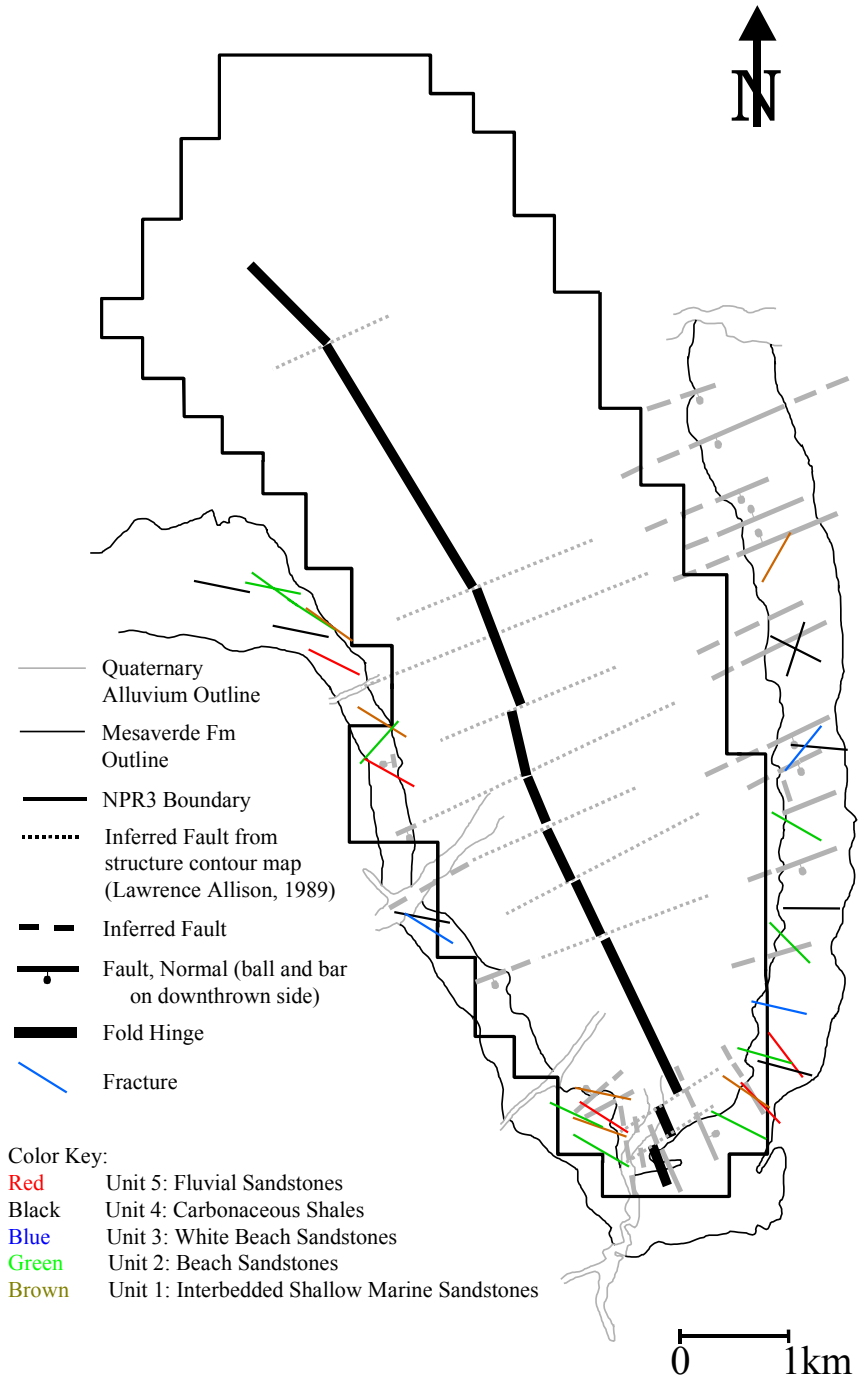

Figure 18: Map of representative fractures striking oblique to the fold hinge at Teapot Dome.

Data collected at a distance from Teapot Dome shows that the oblique set (Figure 19), that strikes predominately NW to WNW, can be found at surrounding locations. Fracture orientation data from Oil Mountain are from Hennings et al. (1998). Three sites at Teapot Dome have hinge-oblique fractures that strike NNE. Fractures striking N to NNE were also observed at three sites at a distance from Teapot Dome, including Oil Mountain.

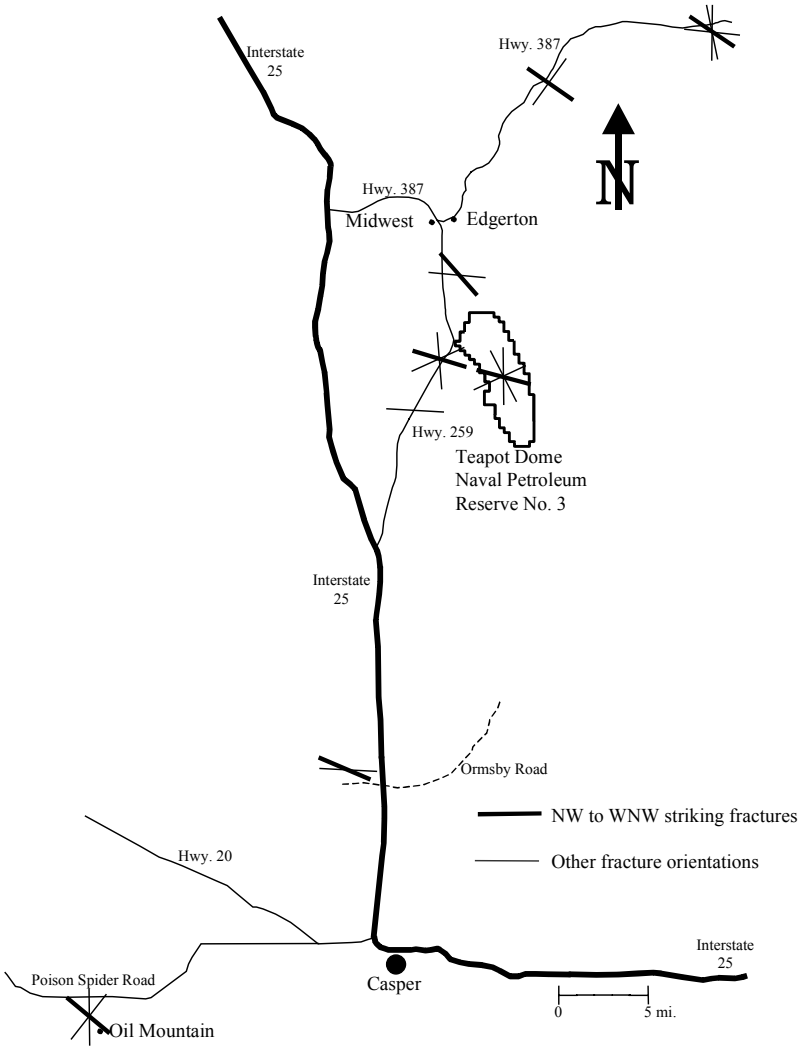

Figure 19: Representative fracture data from locations near and at a distance from Teapot Dome. Oil Mountain data are from Hennings et al. (1998; 2000).

The two dominant, younger, throughgoing fracture sets parallel the two fault sets described previously. Most of these are bed-normal extension fractures. The hinge-perpendicular fracture set was recorded at 35 sites around the anticline. Six additional sites exhibit hinge-perpendicular deformation bands, but no fractures. Fractures and deformation bands of this orientation are best developed along the eastern limb where normal faults are common (compare Figures 15 and 20). The hinge-parallel fracture set is found at 51 sites throughout the fold (Figure 21). Six additional sites exhibit deformation bands without fractures of similar orientation. Locally, bed normal extension fractures are replaced by conjugate shear fractures of the same strike.

Figure 20: Map of representative hinge-perpendicular fractures at Teapot Dome.

Outcrops within the fold hinge are generally absent due to erosion of the fold core. A portion of the hinge remains near the southern exposure of the dome, where it records an increase in fracture density relative to the eastern and western limbs. Spacing between hinge-parallel fractures that are not associated with faults evidence this increase. Eight sites along the southern hinge of the anticline record a mean fracture spacing of 34.7cm (n = 71). Ten sites along the central limbs of the anticline, in contrast, record a mean fracture spacing of 57.3cm (n = 78).

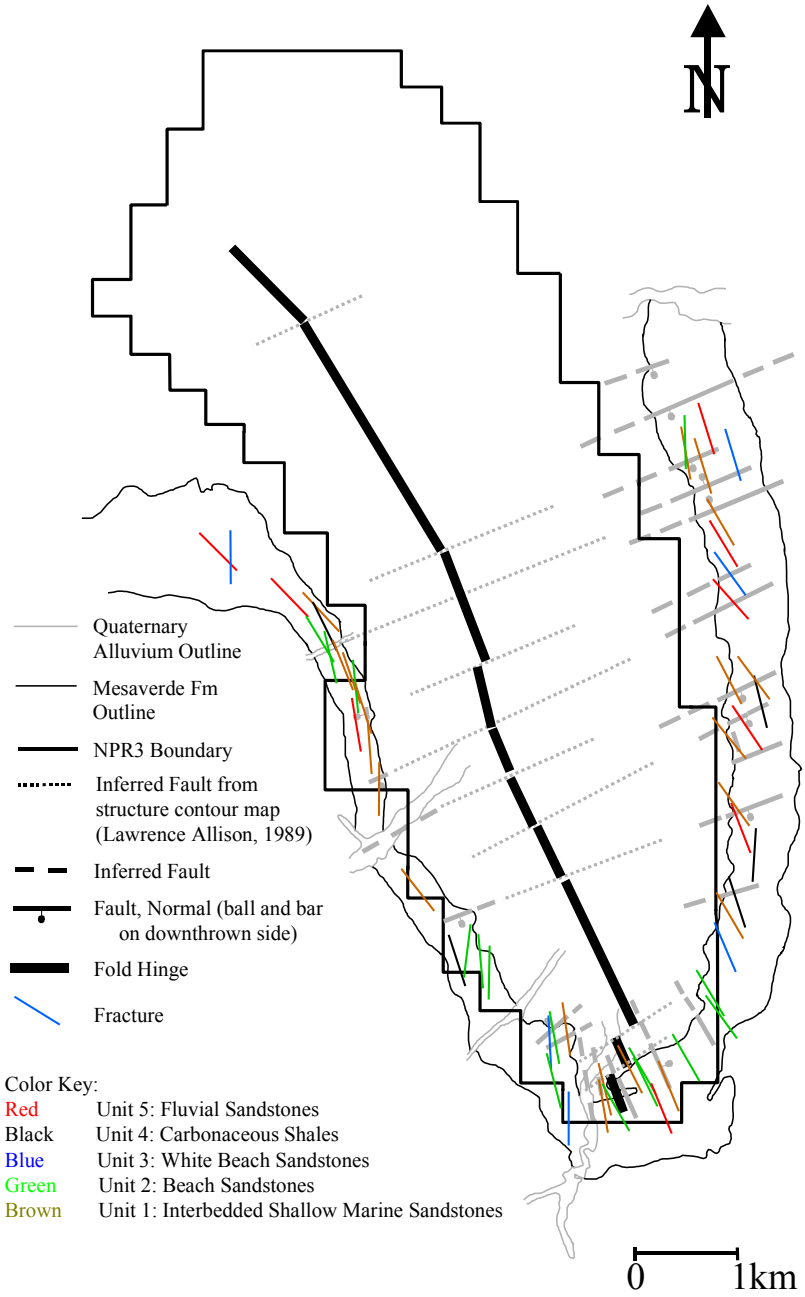

Figure 21: Map of representative hinge-parallel fractures at Teapot Dome.

Where pavement surfaces were large enough, both hinge-parallel and hinge-perpendicular fractures were observed to extend for lengths of up to 100m. At locations where both dominant fracture sets exist they typically meet at T-intersections. The fracture set that does not terminate at the intersection (or junctions) is interpreted to be the oldest fracture set as the younger fracture set would terminate growth at a pre-existing discontinuity (i.e. a pre-existing fracture). At certain outcrops around the anticline, hinge-parallel fractures terminate at hinge-perpendicular fractures (Figure 22). In other locations, hinge-perpendicular fractures terminate at intersections with hinge-parallel fractures. While at other locations the fracture sets

are mutually abutting and therefore interpreted to have formed penecontemporaneously (Figure 22).

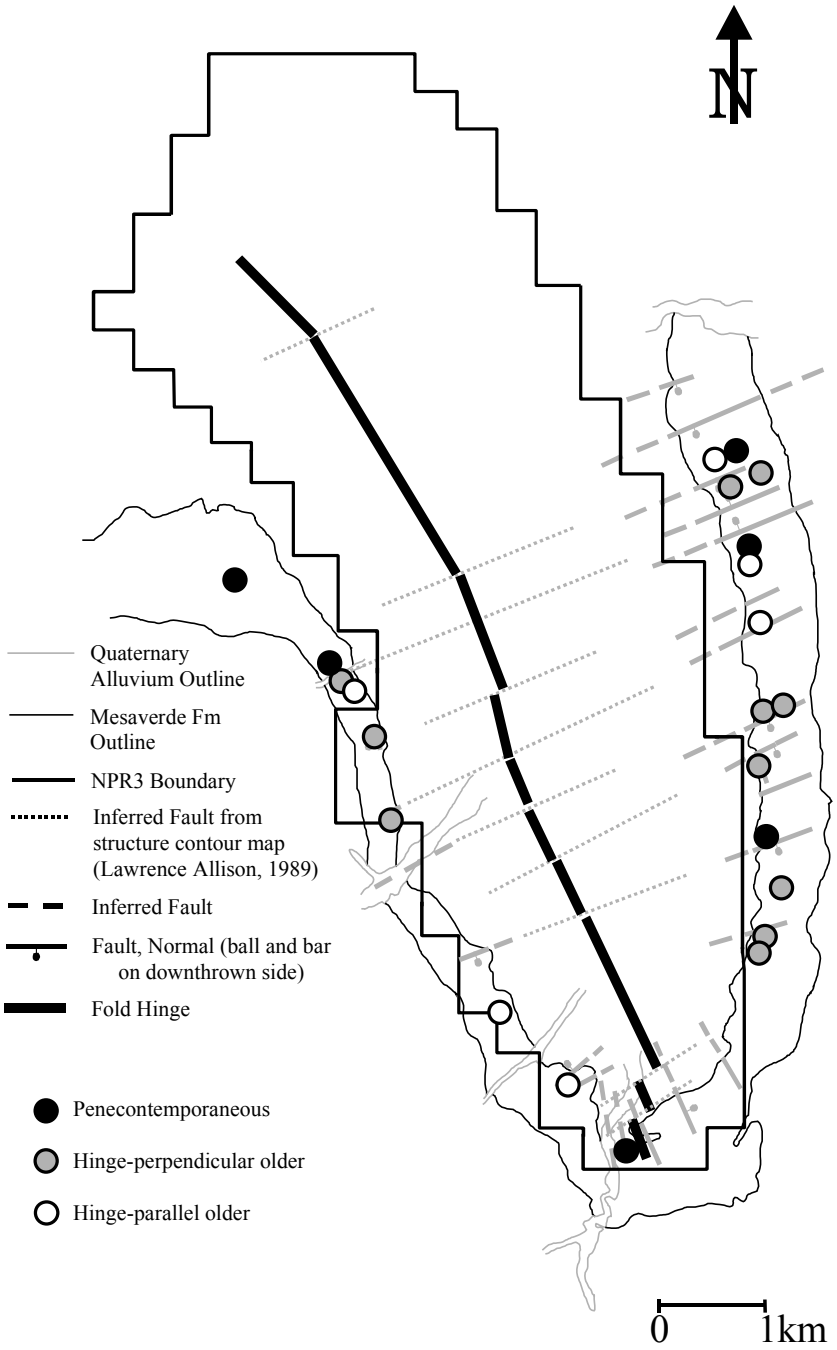

Figure 22: Map illustrating the age relationship of the two dominant fracture sets at locations where such a relative age determination could be made.

Figure 22 shows that there are groupings of locations with similar age relationships for the two dominant fracture sets. Along the southeastern limb hinge-perpendicular fractures are the oldest set. Hinge-perpendicular fractures are also generally the older set near hinge-perpendicular faults. In many locations hinge-perpendicular fractures are spatially related to NE-

striking faults. This relationship is examined further in section 3.3.2 (Spatial relationship between faults and fractures). Hinge-parallel fractures are older along the southwestern limb and in areas between NE-striking faults. These relationships indicate that there may be some partitioning of the two fracture sets and that these dominant sets were forming penecontemporaneously.

3.3.2 Spatial relationship between faults and fractures

As mentioned above, the two dominant fracture sets at Teapot Dome are generally parallel to faults. That is, one set of bed-normal extension fractures is subparallel to hinge-parallel faults, and the second set of bed-normal extension fractures is subparallel to NE-striking faults (and thus perpendicular to the fold hinge). There is also a close spatial relationship between hinge-perpendicular faults and fractures. The density of these fractures increases near the faults (Figure 23).

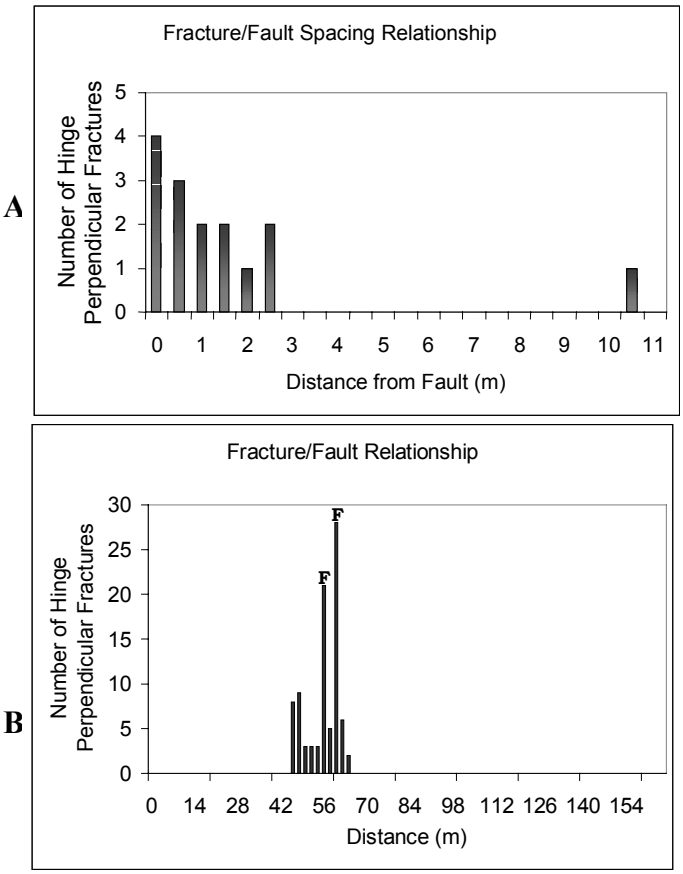

Figure 23: A) Histogram of an outcrop transect starting at, and perpendicular to, a fault on the northeastern limb of Teapot Dome. The histogram shows fractures in the damage zone of the fault increasing in number with proximity to the fault. The fault and fractures strike perpendicular to the fold hinge. B) Histogram of an outcrop transect across a faulted area on the northeastern limb of Teapot Dome. The two F's on the histogram are the locations of hinge-perpendicular faults within the transect. From 0 to 46 m and 68 to 168 m the fractures are hinge-parallel in orientation; from 46 m to 68 m fractures are subparallel to the two hinge-perpendicular faults.

At the location illustrated in Figure 23(B), hinge-perpendicular fractures are only present within a narrow zone adjacent to hinge-perpendicular faults. Hinge-parallel fractures are limited to the area outside this narrow zone, suggesting that the NE-striking faults and fault-related fractures formed first in this area. Unfortunately, the breached nature of Teapot Dome obscures the spatial relationship between hinge-parallel fractures and hinge-parallel faults.

3.4 Discussion

Structures observed within the Cretaceous Mesaverde Formation at Teapot Dome include extension fractures, normal conjugate shear fractures, deformation bands, hinge-parallel normal faults and hinge-perpendicular normal oblique faults. The dominant fracture sets strike roughly parallel to the fault sets. The majority of the fractures are bed-normal extension fractures. These observations agree, in general, with those made by Thom and Speiker (1931). The single exception is in regard to fractures oblique to the fold hinge which they did not recognize. Fisher and Wilkerson (2000) suggested that hinge-oblique fractures could be formed in a fold associated with basement-involved thrusting. Because these hinge-oblique fractures may form early in the folding process they may predate both hinge-parallel and hinge-perpendicular fracture sets and still be related to the folding process. However, at Teapot Dome, the fact the hinge-oblique fractures are older than the other dominant fracture sets and that fractures with similar strikes are recorded at sites away from the anticline suggests they predate folding.

In contrast, hinge-parallel and hinge-perpendicular fracturing and faulting are interpreted to be broadly contemporaneous with basement-involved thrusting and folding at Teapot Dome. This interpretation is based on several observations. Fracture abutting relationships indicate that the two fracture sets were broadly contemporaneous. The dominant fracture sets strike roughly parallel and perpendicular to the fold hinge, suggesting that they are related to the folding event. The fracture sets are parallel and spatially related to the fault sets. Evidence that NE-striking normal-oblique faults are temporally related to folding comes from the observed spatial relationships. These NE-striking faults are oriented roughly perpendicular to the fold hinge, maintaining this relationship even where the hinge axis bends, and die out (or coalesce) toward the SW limb of the anticline. These NE-striking faults may form early in the deformation process as evidenced by the close spatial relationship with hinge-perpendicular fractures and that hinge-perpendicular fractures are older than hinge-parallel fractures near these faults. However, it is important to note that hinge-perpendicular fractures are not universally older than hinge-parallel fractures. In fact the relative age of these fracture sets can be reversed with distance from NE-striking faults.

As mentioned earlier, seismic data show that a basement-involved blind thrust terminates within the lower Paleozoic section. Therefore, regional compression resulted in shortening at the crustal level, manifest in the formation of basement-involved thrusts. The normal-oblique movement recorded on some of the NE-striking faults indicates they may have a transfer fault component related to differential movement across inferred segments of the basement-cored thrust. As noted by Gay (1999), shortening parallel and perpendicular to the fold is required to develop four-way closure. Also using coseismic displacements after the Northridge earthquake of 1994 to model strain in a blind thrust, Unruh and Twiss (1998) determined that horizontal shortening (d_3) was perpendicular to the fold hinge, maximum lengthening (d_1) was horizontal

and parallel to the fold axis and d_2 was vertical. Data from Teapot Dome support both of these concepts. Specifically, hinge-perpendicular fractures and faults record extension parallel to the hinge of Teapot Dome; the fold form itself evidences shortening normal to the hinge. The normal faults, extension fractures and conjugate shear fractures parallel to the fold hinge are interpreted to have accommodated extensional strains related to bending of the brittle sandstone beds. It is also possible that folding was accommodated by flow of the more ductile units within the folded sedimentary section. Further work is required to model possible variations in orientation and type of faults or fractures with increasing depth to basement and decreasing distance to the thrust.

The orientation of structures, such as hinge-parallel and hinge-perpendicular faults and fractures, at Teapot Dome is similar to those described by DeSitter (1956), Murray (1967), Simon et al. (1988), Garrett and Lorenz (1990), Engelder et al. (1997) and Hennings et al., (1998; 2000). Three of the studies, Garrett and Lorenz (1990) and Hennings et al. (1998; 2000) noted fracture sets that predated folding. In most of these studies, the fractures and/or faults striking parallel or perpendicular to the fold hinge were attributed to the folding process.

Structures at Oil Mountain for example are similar to those at Teapot Dome, with fractures striking both parallel and perpendicular to the fold hinge and an increase in fracture density in the southern plunging regions of both anticlines (Hennings et al., 1998; Hennings et al., 2000). However, the hinge-parallel fractures at Oil Mountain were interpreted to predate folding; also the increase in fracture density in southern exposures at Oil Mountain is greater. It is possible the hinge-parallel fractures at Oil Mountain are related to the folding process because the pavement surfaces used as a comparison at a distance from Oil Mountain are still part of the Casper arch, which strikes subparallel to Oil Mountain. Therefore, fractures at both locations may have formed in response to folding. It should be noted however, that the fracture set determined to predate folding at Oil Mountain is subparallel to the fracture set determined to predate folding at Teapot Dome. Therefore, the age relationship between hinge-parallel fracturing and fold formation at Oil Mountain is ambiguous. The difference in fracture density between the two anticlines may be due to Oil Mountain being a tighter fold, evidenced by the forelimb being slightly overturned.

The structures described by Engelder et al. (1997) at Elk Basin anticline are perhaps most similar to those at Teapot Dome. Two fracture sets, one parallel and the other perpendicular to the fold, were documented. Changes in strike of hinge-parallel fractures observed on the forelimb of the anticline were attributed to local faulting as they are at Teapot Dome. At Elk Basin anticline, as at Teapot Dome, a significantly higher percentage of hinge-parallel fractures were observed relative to hinge-perpendicular fractures. Hinge-perpendicular fractures were also observed to extend for considerable lengths in a few areas and to terminate against hinge-parallel fractures in other areas at Elk Basin anticline.

In experimental work by Simon et al. (1988), wherein semibrittle clay cake is deformed over an expanding balloon thus creating a dome, two orthogonal sets of fractures were formed. One set was parallel to the long axis of the dome; the second was perpendicular to that axis. The deep-seated thrust at Teapot Dome would act as the “balloon” forcing the overlying strata (clay cake) to bend.

3.4.1 3-D conceptual model of basement-cored anticlines

The observed fracture trends and interpreted genetic relationships from Teapot Dome and similar folds have been used to create a conceptual model of fault and fracture development in an anticline above a basement-cored thrust. The two main through-going fracture sets incorporated into this 3-D model are: 1) bed-normal extension fractures striking subparallel to NE-striking oblique normal faults and perpendicular to the fold hinge, and 2) bed-normal extension fractures and normal faults striking parallel to the fold hinge (Figure 24). The fracture set determined to predate folding at Teapot Dome is not incorporated into this conceptual model, as pre-existing regional fracture sets will vary in orientation with location.

A comparison between this and an earlier conceptual model (Stearns and Friedman, 1972) that describes fracturing associated with folding (based on data from Teton anticline) shows significant differences as well as some similarities in the fracture patterns (compare Figures 14 and 24). Conjugate fractures in the Stearns and Friedman (1972) model are oriented such that the bisector of the acute angle is parallel to the plane of bedding, while the Teapot Dome model illustrates conjugate fractures that have a vertical bisector to the acute angle. These shear fractures obliquely transect the anticline in the Stearns and Friedman (1972) model. The shear fracture sets in the Teapot Dome model strike either parallel or perpendicular to the hinge. However, the extension fractures in both models strike both parallel and perpendicular to the fold hinge in the vicinity of the culmination. Near the plunging nose of the anticline, where bedding strike is not parallel to the fold hinge, differences in extension fracture patterns become apparent. Bedding strike rotates through a 180^{o} turn around the hinge at this point. Here the Stearns and Friedman (1972) fracture sets, by remaining parallel to bedding strike, change orientation with respect to the fold hinge, whereas the fracture sets within the Teapot Dome model remain parallel and perpendicular to the fold hinge (compare Figures 14 and 24). Each of these observations suggests a significant difference in permeability anisotropy between models, as noted in the following section.

It is important to note that there may be a structural explanation for the differences between these two 3-D models. The two anticlines are distinctly different both in terms of the depth of the thrust relative to the fractured strata on which the models are based and in the type of folding process. Teapot Dome is situated above a deep-seated, basement-cored thrust. The sedimentary layers over the area of faulting are interpreted to be essentially draped over the thrust. In contrast, Teton anticline is cored by a thin-skinned thrust that propagated through the sedimentary section. As described by Sinclair (1980), the Teton anticlines, separated by an unfaulted syncline, are essentially buckle folds in the form of a wave train over the thin-skinned thrust. It may be that bedding-parallel shortening is significantly greater in the latter case as evidenced by conjugate fractures with a horizontal (parallel to bedding) bisector to the acute angle. This may also hold true for the fault propagation and fault-bend folds documented by Cooper (1990) and the Palm Valley fold studied by Berry et al. (1996), wherein fracture orientations representative of the Stearns and Friedman (1972) model where recorded.

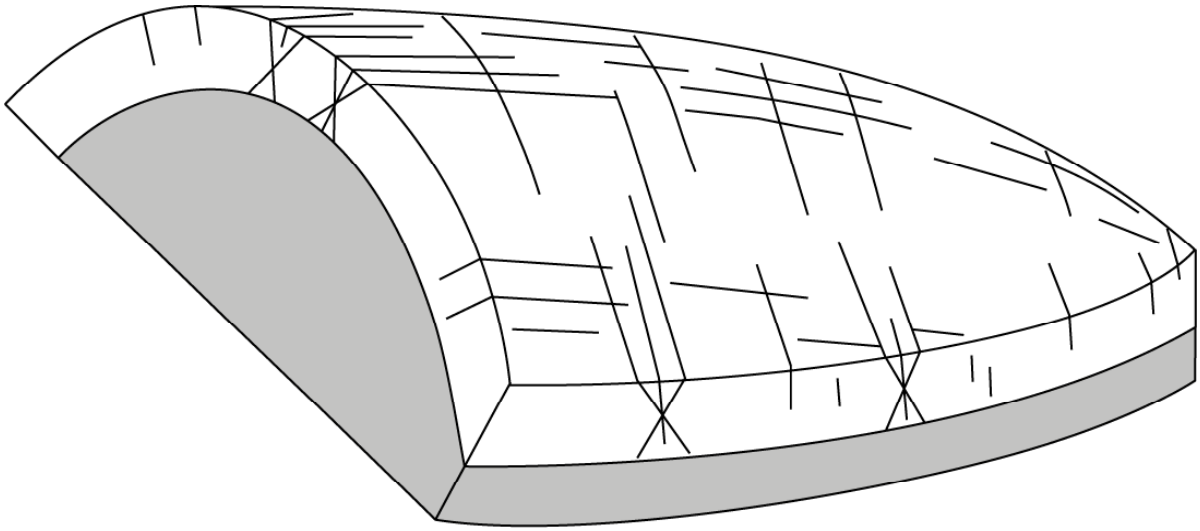

Figure 24: Conceptual 3-D model of fracture patterns developed at Teapot Dome.

Implications of these fracture patterns on fluid flow include: significant permeability anisotropy, with maximum permeability generally along the fold hinge due to numerous hinge-parallel fractures near the apex of the anticline; NE-striking normal faults and associated fractures may cause the direction of maximum permeability to be locally perpendicular to the fold hinge; and intersections between hinge-perpendicular and hinge-parallel faults and fractures may allow for increased production.

Conversely, brittle sandstones at Teapot Dome indicate lengthening in the area of flexure (drape) over the deep-seated thrust as evidenced by conjugate fractures and faults with a vertical bisector to the acute angle. The majority of folds that have fracture patterns similar to those at Teapot Dome are those associated with deep-seated blind thrusts. It should also be noted that Stearns (1964) observed a conjugate fracture set with a vertical bisector to the acute angle at Teton anticline, which was not considered a dominant fracture set by Stearns and Friedman (1972). This fracture set was attributed to folding; bedding was visualized as a bent beam, wherein the upper arc would be an area of extension but the lower arc would be an area of shortening.

3.4.2 Fluid flow implications

There are a number of implications of the fracture patterns that are incorporated into the conceptual fracture model (Figure 24). Since the dominant set of throughgoing fractures is parallel to the fold hinge, significant permeability anisotropy is expected, with maximum permeability generally parallel to the fold hinge across the entire anticline. Areas of greatest change in dip of bedding (i.e., the fold hinge) are areas of increased fracture density, with fractures generally parallel to the fold hinge. The increase in hinge-parallel fractures near the hinge of the anticline should be associated with an increase both in permeability and permeability anisotropy. NE-striking normal faults and associated fractures may locally cause the direction of maximum permeability to be perpendicular to the fold hinge. This is particularly

relevant to the culmination of the fold where NE-striking faults are numerous. However, even here the area between NE-striking faults can be dominated by hinge-parallel fractures. Therefore, the location of a specific well and its proximity to a fault zone will determine the relative amount of hinge-perpendicular vs. hinge-parallel fluid flow. Intersections of hinge-perpendicular with hinge-parallel faults and associated fractures should be areas of enhanced permeability, where increased interconnectivity may allow for locally increased production. The permeability anisotropy will depend on the number of faults and fractures of each set and degree of interconnectivity, and will thus vary from site to site.

A preexisting fracture and deformation band set oblique to the fold hinge is specific to Teapot Dome. This fracture and deformation band set is found throughout the fold and in all lithologies and will have an influence on fluid flow. Doll et al. (1995) describe this fracture set, which strikes N65^{o}W, as providing the most significant flow directionality with respect to water response and rapid oil response time during steam flooding.

It should be noted that mineralization within the faults and fractures will play an important role in all of the previous assessments. Highly mineralized fractures and faults will reduce the overall permeability within a volume of rock. They would still result in a direction of maximum permeability parallel to the mineralized fault or fracture set, but in this case, the zone of highest permeability would be the matrix and not the fracture or fault plane. The majority of fractures and faults studied were relatively unmineralized. However, localized areas of moderate mineralization were observed. Detailed information regarding mineralization is included in Section 2: Lithologic Controls.

3.5 Conclusions

Fractures and faults associated with folding within the Cretaceous Mesaverde Formation at Teapot Dome display variable patterns associated with structural position, including: 1) fracture density increases near faults, 2) conjugate fractures and deformation bands, oriented such that they have a vertical bisector to the acute angle, and faults striking subparallel to the axis of the anticline, are common in the exposed hinge of the anticline, 3) NE-striking normal-oblique faults and associated fractures are generally perpendicular to the fold hinge, and are more closely spaced near the culmination of the dome, and 4) extension fractures and faults that are parallel to the fold hinge, and are more closely spaced near the hinge.

The deformation process that formed the faults, fractures and fold is interpreted to have been a dynamic interactive system, wherein progressive folding was driven by displacement on the basement-involved thrust fault. Variable displacement along the thrust front was accommodated by transfer faults (the NE-striking normal oblique faults) at roughly right angles to the thrust fault. These faults also accommodated a component of extension associated with bending of beds across the fold. Normal faulting perpendicular to the fold hinge accommodates the fold form in this direction. Hinge-parallel normal faults formed to accommodate the fold form and are roughly parallel to the thrust fault. In addition, fractures formed in brittle sandstones and carbonaceous shales in response to the fold form (driven by the basement thrust) and to displacements along faults (also driven by the basement thrust) while more ductile marine shales are interpreted to have responded to shortening through flow.

These observations indicate that maximum horizontal permeability associated with these fractures and faults will generally be hinge-parallel, especially near the apex of the anticline. Localized areas of maximum permeability that are perpendicular to the fold hinge may be found within the damage zones of NE-striking normal faults. A preexisting NW-WNW fracture set specific to Teapot Dome will also influence fluid flow. This set was observed in outcrop and inferred by Doll et al. (1995) from data collected during steam flooding of Shannon reservoirs.

Given the importance of correctly modeling permeability and fluid flow anisotropy it is essential to use the most appropriate reservoir analog. This study provides a conceptual model of fault and fracture distribution that is in many ways similar to previous descriptions of basement-involved anticlines, including a previous study at Teapot Dome (Thom and Speiker, 1931; DeSitter, 1956; Murray, 1967; Garrett and Lorenz, 1990; Cooper, 1992; Engelder et al., 1997; Hennings et al., 1998; Unruh and Twiss, 1998; Hennings et al., 2000). The model is, however, significantly different from Stearns's and Friedman's (1972) model, which has been widely applied to all anticlines regardless of the folding process. We believe that the model developed from the Teapot Dome data set is best applied to basement-cored structures while the Stearns and Friedman (1972) model would be a better analog for folds developed above thin-skinned thrusts. In other words, fracture analogs are best applied with knowledge of the tectonic setting of the structure of interest. Using the wrong model can result in a poorly designed secondary recovery system, wherein early breakouts occur and/or production is not enhanced.

4.0 APPLICATION (RECOMMENDATION FOR A HORIZONTAL WELL AZIMUTH)

During the spring of 2000 the Rocky Mountain Oilfield Testing Center (RMOTC) requested a recommendation for a horizontal well azimuth at Teapot Dome. This section summarizes the available outcrop and core data pertinent to the design of this horizontal wellbore azimuth. The given limitations are that the well would be drilled in Section 23 at the southern end of the anticline, and that it would target fracture zones of the Steele and Niobrara shale formations. The well was not drilled due to insufficient funding, but the following analysis is offered for future reference.

4.1 Outcrop Evidence

4.1.1 Fractures

There is a strong hinge-parallel, north-northwest fracture and fault set in the region of Section 23 at the southern plunge of the anticline (Figure 25). Hinge-parallel, north-northwest striking fractures are better developed in this region than in other parts of the anticline, and locally cut through numerous bedding planes to extend vertically for tens of feet rather than being limited vertically by bedding as they are elsewhere. The east-west fractures that are common in other parts of the anticline are poorly developed in Section 23.

Outcrop data show that the age relationship between the hinge-parallel and hinge-normal fractures varies around the Teapot Dome structure. This suggests that the two fracture sets were

forming penecontemporaneously, and that the two horizontal stresses exchanged orientations from place to place and perhaps through time as well. Hinge-parallel faults and fractures dominate the structural fabric at the southern plunge of the anticline, suggesting that extension normal to the hinge was the most important strain mechanism in this structural domain. Therefore, the maximum horizontal compressive stress in this area is most likely to strike parallel to the hinge of the anticline.

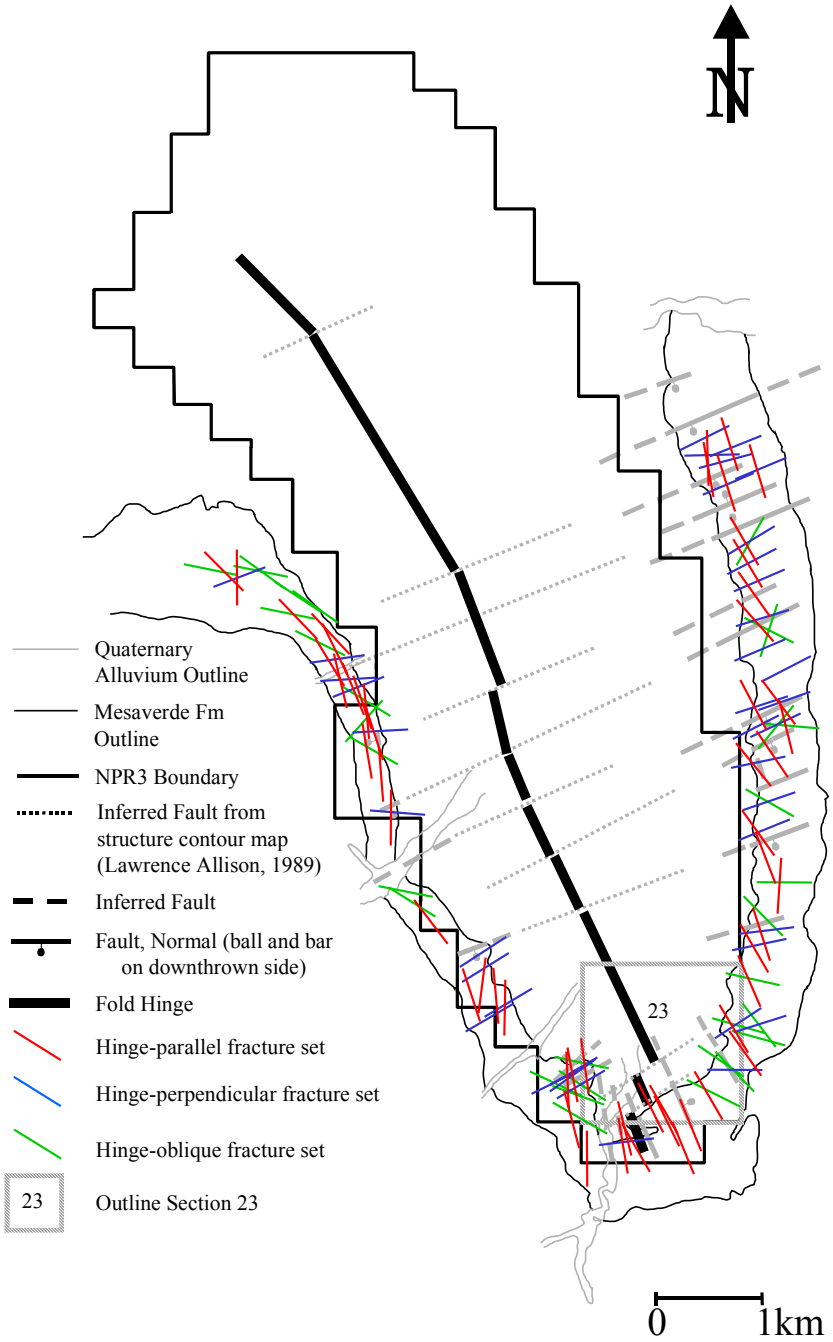

Figure 25: Map showing the three primary fracture sets relative to Section 23. Section 23 is in the southern plunging region of the anticline.

4.1.2 NNW Faults

There are several faults (shown in red in Figure 26) that strike parallel to the anticlinal axis in the region of the southern plunge of the Teapot Anticline. One of these faults forms the canyon leading through the Mesaverde rimrock to the terminal. It is poorly defined but appears to have increasing throw northward.

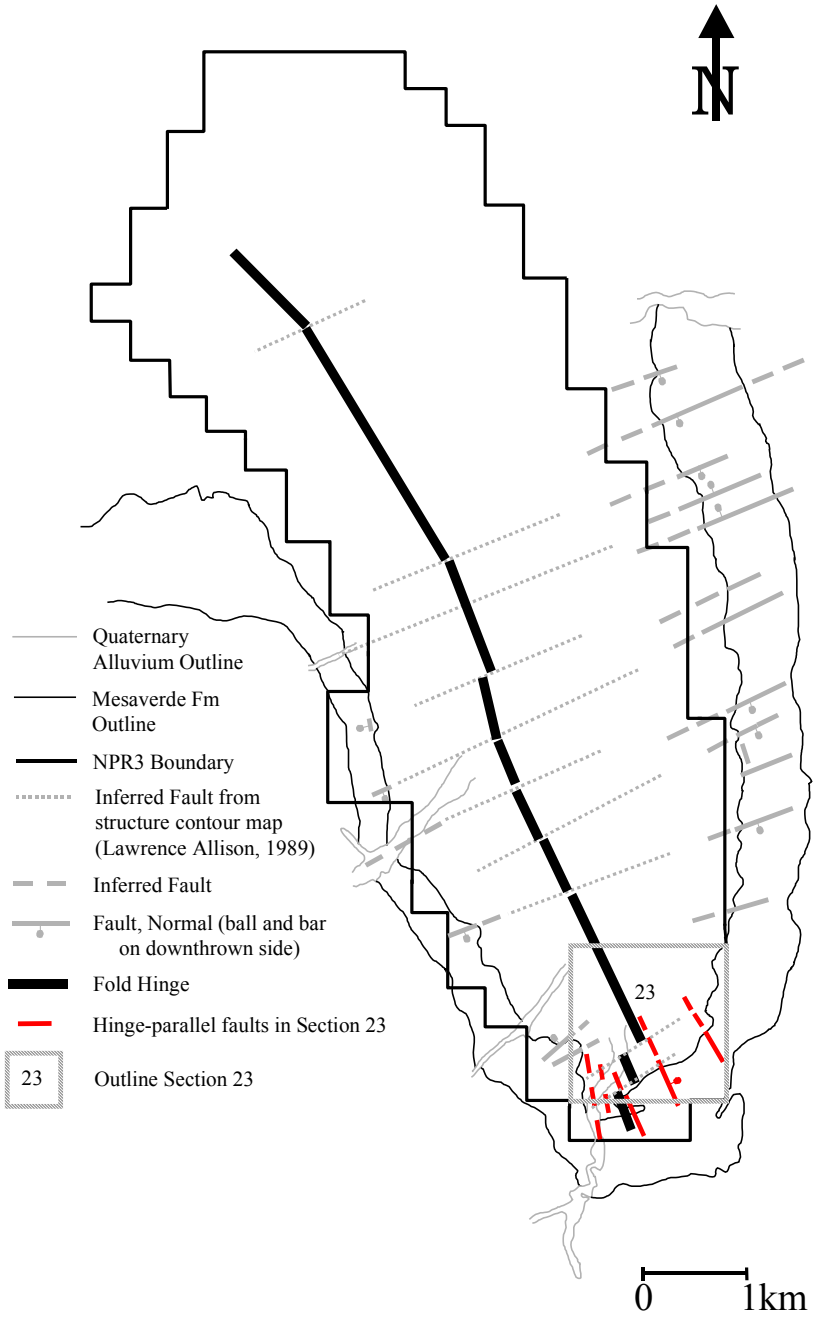

Figure 26: Map highlighting the hinge-parallel faults within Section 23.

The other major has a hinge-parallel strike and is located about half a kilometer to the east of the canyon. This fault can be traced through the Mesaverde strata along a strike of 337° – 157° (N23°) for several hundred meters. The fracture-weakened rock in this fault creates an erosional notch or gap in the thicker Mesaverde sandstones. To the south it is a down-to-the-east normal fault zone dipping 68° to the east. Throw appears to increase to the north.

When projected northward out into the core of the anticline, the strike of this fault aligns with the 55StX23 well. Fault/fracture-enhanced permeability and porosity may account for the high production rates from this well. The north-northwesterly strike and east-northeast dip of the fault would explain why the offset well, including 54StX23 drilled on the location directly to the north of 55StX23, did not encounter similar reservoir conditions.

These two north-northwest striking faults would make good targets for a deviated well assuming that they have not been depleted by other wells. The eastern fault is the better defined of the two, whereas, the western fault may be the larger one. A wellbore azimuth oriented within plus or minus 30 degrees of normal to these faults (i.e. between 37° and 97° if deviated to the northeast, or between 217° and 277° if deviated to the southwest) would have an excellent chance of penetrating these structures. East-northeast or west-southwest well azimuths would traverse the better-developed hinge-parallel fracture system along the plunging hinge of the anticline.

4.1.3 NE Faults

Hinge-normal faults are common in the central portion (i.e. culmination) of the anticline, where calcite-mineralized veins can be traced through gullies cut into the shales exposed at the surface. Hinge-normal is also one of the three subsurface fracture directions inferred for Teapot Dome by Doll et al. (1995) from steam flood response data. Finally, using indirect surface geochemical techniques such as surface hydrocarbons, Eh, pH, soil electrical conductivity, iodine, and bacteria, Fausnaugh and LeBeau (1997) observed trends also suggesting NE-striking faults.

Hinge-normal fractures may not provide a sufficient target for a hinge-parallel wellbore azimuth as few NE-striking faults are observed in outcrop within section 23. Specifically, only two hinge-normal faults were observed on the western edge of section 23 (Cooper, 2000). These faults strike 45° and 60°, and consist of fault zones 20-30 meters wide with normal, dip-slip movement (down to the north or graben) of less than 5 meters. The extent of these faults into the subsurface to the east is uncertain, although they do not appear to have counterparts on the eastern limb. A well drilled specifically to intersect these faults would have a wellbore azimuth of 300° – 330°.

4.1.4 Deformation Bands

Deformation bands formed rather than fractures in certain high-porosity sandstones of the Mesaverde Formation. These structures are shear bands of crushed sand grains that form conjugate planes within the rock, which severely restrict permeability. The high-porosity sandstones have poor reservoir potential due to these deformation bands, which compartmentalize the rock into non-communicating sections. However, these features are not

likely to be present in the target shale zones.

4.2 Core Evidence

About 300ft of core from the Shannon Sandstone in nine wells at Teapot Dome were examined during the week of 2/10/97 (see section 2.4.4). These cores are slabbed and in good condition but they are not oriented. The core show that the typical, heavily bioturbated Shannon sandstones are not fractured, but that the rare associated thin beds of clean, unburrowed sandstones have numerous natural fractures that are partially mineralized with calcite.

High-angle, dip-shear planes are present within the associated shale intervals, indicating significant deformation has occurred within the non-reservoir intervals. Since the sandy reservoir intervals were preferentially cored, it is difficult to say how pervasive these faults are in the shale intervals that bound the reservoirs.

Unoriented core data do not lend themselves to aiding in determining an optimum azimuth for a horizontal well. However, they indicate that fractures and faults are present in both the sandstones and associated shales. Historical production data suggest that the larger faults in the shales are potential reservoir targets.

4.3 Recommendations

Fractures and faults with the best reservoir potential in Section 23 (at the southern plunge of Teapot Dome) trend north-northwest. The maximum horizontal compressive stress also probably trends in this hinge-parallel direction. The azimuth of a horizontal wellbore designed to intersect these structures would be within plus or minus 30^{o} of either east-northeast or west-southwest (67^{o} or 247^{o}). Subordinate faults found only on the western limb of the anticline in this area trend northeast, and a well designed to access these structures in the subsurface would have and azimuth of approximately northwest. Faults are present in shale cores and may indicate the potential for reservoir strata in these formations. High-porosity sandstones, however, are prone to deformation banding which degrades reservoir quality when present.

5.0 RECOMMENDATIONS FOR FUTURE WORK

The 3-D conceptual model developed here should not be applied equally to all anticlines. Although the model does provide another useful tool to help determine fluid flow directionality in one type of fractured reservoir, several questions remain unresolved: 1) How deep into the subsurface can the model adequately predict fracture and fault orientations and distributions? Further study of fractures at basement-cored anticlines with exposures of strata lower in the section, such as work done by Hennings et al. (1998; 2000), may help. 2) Are the qualitative permeability anisotropy observations accurate? These could be tested by comparing in-situ well tests with a fluid flow simulation based on Teapot Dome stratigraphy and structure, as provided from well data, seismic sections, and the 3-D conceptual model. 3) How tight can the anticline be before the model becomes invalid? This may require an outcrop study of anticlines with limbs that dip at angles higher than the maximum 30 degree dip angle observed at Teapot Dome.

Other important considerations in comparing various sites are differences or similarities in lithology, mechanical stratigraphy and tectonic setting.

Further core analysis would be a natural next step in evaluating fractures at Teapot Dome. The NPR #3 facility has a very good core library on premise. This data would provide a better characterization of fractures and permeability anisotropy in subsurface reservoirs.

Recently the Rocky Mountain Oil Field Testing Center acquired a 15 square mile 3-D seismic data cube over Teapot Dome. Interpretation of this cube would answer questions concerning the along strike and vertical extent of faults observed in outcrop. Questions could also be addressed concerning the change of structural curvature with depth and where the transition between vertical and horizontal shortening occurs.

6.0 SUMMARY

Fractures, deformation bands and faults were observed to controlled by lithology as well as structure. Structure primarily controls spacing and orientation. While lithology influences spacing, vertical extent and the very nature of deformation (i.e. will the unit deform through fracturing or the formation of deformation bands).

A 3-D conceptual model of fractures associated with basement-cored anticlines was developed from extensive work on Mesaverde Formation outcrops at Teapot Dome, Wyoming. The outcrop data show two primary fracture and fault sets (which were incorporated into the model) associated with folding. One set is parallel to the fold hinge the second set is perpendicular to the fold hinge. A third set, which predates folding, is oblique to the fold hinge.

Utilization of the developed model as an analog, applied with the concepts of structural and lithologic controls, can provide a first order approximation of probable permeability anisotropy in areas where large amounts of data are unavailable. Understanding (even partially) the directionality of fluid flow in a hydrocarbon reservoir will make both initial production and enhanced recovery more profitable.

7.0 ACKNOWLEDGEMENTS

This work was sponsored by the National Petroleum Technology Office of the National Energy Technology Laboratory (US Department of Energy), Tulsa, OK. Our thanks to Bob Lemmon contract manager for this project. This work has also been supported by the Rocky Mountain Oilfield Testing Center and the Naturally Fractured and Stress Sensitive Reservoir Consortium under Larry Teufel at New Mexico Tech. We also gratefully acknowledge and thank the landowners and operators (Tom Allemand and family, Bill and Mary Owens, John Beaton, and Leland Bertagnole) surrounding NPR #3 for permission to describe and measure the outcrops on their property. Thanks also to everyone associated with NPR#3 and the Rocky Mountain Oilfield Testing Center especially Mark Milliken. Sandia is a multiprogram laboratory

operated by Sandia Corporation, a Lockheed Martin Company, for the United States Department of Energy under contract DE-AC04-94AL85000.

8.0 REFERENCES

Antonellini, M., and Aydin, A., 1994, Effect of faulting on fluid flow in porous sandstones: Petrophysical properties: American Association of Petroleum Geologists Bulletin, v. 78, p. 355-377.

Antonellini, M., and Aydin, A., 1995, Effect of faulting on fluid flow in porous sandstones: Geometry and spatial distribution: American Association of Petroleum Geologists Bulletin, v. 79, p. 642-671.

Antonellini, M., Aydin, A., and Pollard, D. D., 1994, Microstructure of deformation bands in porous sandstones at Arches National Park, Utah: Journal of Structural Geology, v. 16, p. 941-959.

Aydin, A., 1978, Small faults formed as deformation bands in sandstone: Pure and Applied Geophysics, v. 116, p. 913-930.

Bai, T., and Pollard, D. D., 2000, Fracture spacing in layered rocks: a new explanation based on the stress transition: Journal of Structural Geology, v. 22, p. 43-57.

Berg, R. R., 1962, Mountain flank thrusting in Rocky Mountain Foreland, Wyoming and Colorado: American Association of Petroleum Geologists Bulletin, v. 46, p. 2019-2032.

Berry, M. D., Stearns, D. W., and Friedman, M., 1996, The development of a fractured reservoir model for the Palm Valley gas field: Australian Petroleum Production and Exploration Association Journal, v. 36, no. 1, p. 82-103.

Blackstone, D. L., Jr., 1940, Structure of the Pryor Mountains, Montana: Journal of Geology, v. 48, p. 590-618.

Blackstone, D. L., Jr., 1980, Foreland deformation: compression as a cause: University of Wyoming Contributions in Geology, v. 18, p. 83-101.

Bogdanov, A. A., 1947, The intensity of cleavage as related to the thickness of beds (in Russian): Soviet Geology, no. 16.

Caine, J. S., Evans, J. P., and Forster, C. B., 1996, Fault zone architecture and permeability structure: Geology, v. 24, no. 11, p. 1025-1028.

Committee on Fracture Characterization and Fluid Flow, 1997, Rock Fracture and Fluid Flow: Washington, D.C., National Academy Press, p. 551.

Cooper, M., 1992, The analysis of fracture systems in subsurface thrust structures from the Foothills of the Canadian Rockies, *in* McClay, K. R., ed., Thrust Tectonics, London, Chapman and Hall, p. 391-405.

Cooper, S. P., 2000, Deformation within a basement-cored anticline Teapot Dome, Wyoming [M.S. thesis]: New Mexico Institute of Mining and Technology, 274 p.

Curry, W. H., 1977, Teapot Dome - past, present and future: American Association of Petroleum Geologists Bulletin, v. 61, p. 671-697.

DeSitter, L. U., 1956, Structural Geology, McGraw-Hill Series in the Geological Sciences: New York, McGraw-Hill, 552 p.

DeSitter, L. U., 1964, Variation in tectonic style: Bulletin of Canadian Petroleum Geology, v. 12, no. 2, p. 263-278.

Doelger, M. J., Mullen, D. M., and Barlow & Haun, I., 1993, Nearshore marine sandstone, Atlas of Major Rocky Mountain Gas Reservoirs: Socorro, NM, New Mexico Bureau of Mines and Mineral Resources, p. 54-55.

Doll, T. E., Luers, D. K., Strong, G. R., Schult, R. K., Sarathi, P. S., Olsen, D. K., and Hendricks, M. L., 1995, An update of steam injection operations at Naval Petroleum Reserve No. 3, Teapot Dome Field, Wyoming: A shallow heterogeneous light oil reservoir, SPE 30286, *in* International Heavy Oil Symposium, Calgary, Alberta, Canada, p. 1-20.

Dunn, D. D., LaFountain, L. J., and Jackson, R. E., 1973, Porosity dependence and mechanism of brittle fracture in sandstones: Journal of Geophysical Research, v. 78, p. 2403-2417.

Elkins, L. F., and Skov, A. M., 1960, Determination of fracture orientation from pressure interference: Petroleum Transactions, American Institute of Mining Engineers, v. 219, p. 301-304.

Engelder, T., 1974, Cataclasis and the generation of fault gouge: Geological Society of America Bulletin, v. 85, p. 1515-1522.

Engelder, T., Gross, M. R., and Pinkerton, 1997, An analysis of joint development in thick sandstone beds of the Elk Basin anticline, Montana-Wyoming, *in* Hoak, T. E., Klawitter, A. L., and Blomquist, P. K., eds., Fractured reservoirs: characterization and modeling: Rocky Mountain Association of Geologists Guidebook, p. 1-18.

Fassett, J. E., 1991, Oil and gas resources of the San Juan basin, New Mexico and Colorado, *in* Gluskoter, H. J., Rice, D. D., and Taylor, R. B., eds., Economic Geology, U.S.: The Geology of North America, Geological Society of America, p. 357-372.

Fausnaugh, J. M., and LeBeau, J., 1997, Characterization of shallow hydrocarbon reservoirs using surface geochemical methods: American Association of Petroleum Geologists Bulletin, v. 81, no. 7, p. 1223.

Fisher, M. P., and Wilkerson, M. S., 2000, Predicting the orientation of joints from fold shape: Results of pseudo-three-dimensional modeling and curvature analysis: Geology, v. 28, no. 1, p. 15-18.

Fjaer, E., Holt, R. M., Horsrud, P., Raaen, A. M., and Risnes, R., 1992, Petroleum related rock mechanics: New York, Elsevier Science Publishing Company Inc., 388 p.

Fox, J. E., Dolton, G. L., and Clayton, J. L., 1991, Powder River Basin, *in* Gluskoter, H. J., Rice, D. D., and Taylor, R. B., eds., Economic Geology, U.S.: Geological Society of America, The Geology of North America, P-2, p. 373-390.

Garrett, C. H., and Lorenz, J. C., 1990, Fracturing along the Grand Hogback, Garfield County, Colorado, *in* Bauer, P. W., Lucas, S. G., Mawer, C. K., and McIntosh, W. C., eds., New Mexico Geological Society Guidebook, 41st Field Conference, Southern Sangre de Cristo Mountains, New Mexico, p. 145-150.

Gay, S. P., Jr., 1999, An explanation for "4-way closure" of thrust-fold structures in the Rocky Mountains, and implications for similar structures elsewhere: The Mountain Geologist, v. 36, no. 4, p. 235-244.

Gill, J. R., and Cobban, W. A., 1966, Regional unconformity in Late Cretaceous, Wyoming: United States Geological Survey Professional Paper 550-B, p. B20-B27.

Gribbin, D. J., 1952, Completion report exploratory well no. 1-G-10 at Naval Petroleum Reserve No. 3, Natrona County, Wyoming, A&E Contract NOy-29897, Spec. No. 31556.

Gries, R., 1983, Oil and gas prospecting beneath Precambrian of foreland thrust plates in Rocky Mountains: American Association of Petroleum Geologists Bulletin, v. 67, p. 1-28.

Gries, R. R., and Dyer, R. C., 1985, Seismic exploration of the Rocky Mountain foreland structures: Denver, Rocky Mountain Association of Geologists and the Denver Geophysical Society, p. 298.
Gross, M. R., 1993, The origin and spacing of cross joints: examples from the Monterey Formation, Santa Barbara Coastline, California: Journal of Structural Geology, v. 15, no. 6, p. 737-751.
Haneberg, W. C., 1995, Steady state groundwater flow across idealized faults: Water Resources Research, v. 31, no. 7, p. 1815-1820.
Harding, T. P., and Lowell, J. D., 1979, Structural styles, their plate-tectonic habitats, and hydrocarbon traps in petroleum provinces: American Association of Petroleum Geologists Bulletin, v. 63, no. 7, p. 1016-1058.
Harris, J. F., Taylor, G. L., and Walper, J. L., 1960, Relation of deformation fractures in sedimentary rocks to regional and local structure: American Association of Petroleum Geologists Bulletin, v. 44, no. 12, p. 1853-1873.
Hennings, P. H., Olsen, J. E., and Thompson, L. B., 2000, Combining outcrop data and three-dimensional structural models to characterize fractures reservoirs: An example from Wyoming: American Association of Petroleum Geologists Bulletin, v. 84, no. 6, p. 830-849.
Hennings, P. H., Olson, J. E., and Thompson, L. B., 1998, Using outcrop data to calibrate 3-D geometric models for prediction of reservoir-scale deformation: An example from Wyoming, *in* Fractured reservoirs: practical exploration and development strategies, Symposium Proceedings, p. 91-95.
Hobbs, D. W., 1967, The formation of tension joints in sedimentary rocks: an explanation: Geological Magazine, v. 104, no. 6, p. 550-556.
Hoshino, K., 1974, Effect of porosity on the strength of clastic sedimentary rocks, *in* Advances in Rock Mechanics, Proc. 3rd Int. Soc. Rock Mech., Denver, Colorado, p. 511-516.
Huang, Q., and Angelier, J., 1989, Fracture spacing and its relation to bed thickness: Geological Magazine, v. 126, no. 4, p. 355-362.
Huntoon, P. A., and Lundy, D. A., 1979, Fracture-controlled ground-water circulation and well siting in the vicinity of Laramie, Wyoming: Ground Water, v. 17, p. 463-469.
Jamison, W. R., and Stearns, D. W., 1982, Tectonic deformation of Wingate Sandstone, Colorado National Monument: American Association of Petroleum Geologists Bulletin, v. 66, p. 2584-2608.
Ji, S., and Saruwatari, K., 1998, A revised model for the relationship between joint spacing and layer thickness: Journal of Structural Geology, v. 20, no. 11, p. 1495-1508.
Kuenen, P. H., 1958, Experiments in geology, *in* Macgregor, M., and Weir, J., eds., Transactions Geological Society Glasgow: Glasgow, Geological Society of Glasgow, p. 1-28.
Ladeira, F. L., and Price, N. J., 1981, Relationship between fracture spacing and bed thickness: Journal of Structural Geology, v. 3, p. 179-183.
LeBeau, J., 1996, Preliminary geological characterization of the Dakota Formation, Naval Petroleum Reserve #3, Midwest, Wyoming, RMOTC/Halliburton multilateral test, October 1996: Rocky Mountain Oilfield Technology Center Internal Report, p. 25 p. plus appendices.

Lorenz, J. C., 1997a, Heartburn in predicting natural fractures: The effects of differential fracture susceptibility in heterogeneous lithologies, *in* Hoak, T. E., Klawitter, A. L., and Blomquist, P. K., eds., Fractured reservoirs: Characterization and modeling: Rocky Mountain Association of Geologists Guidebook, p. 57-66.

Lorenz, J. C., 1997b, Natural fractures and in-situ stresses in the Teapot Dome: Proposal for development of an analog to Rocky Mountain anticlines, *in* Wyoming Geological Association 48th Annual Field Conference Technical Abstracts, Casper, Wyoming, p. 5-6.

Lorenz, J. C., and Finley, S. J., 1989, Differences in fracture characteristics and related production: Mesaverde Formation, Northwestern Colorado: Society of Petroleum Engineers Formation Evaluation, v. 4, p. 11-16.

Lorenz, J. C., and Finley, S. J., 1991, Regional fractures II: Fracturing of Mesaverde Reservoirs in the Piceance Basin, Colorado: American Association of Petroleum Geologists Bulletin, v. 75, p. 1738-1757.

Lorenz, J. C., and Hill, R. E., 1991, Subsurface fracture spacing: comparison of inferences from slant/horizontal core and vertical core in Mesaverde reservoirs: Society of Petroleum Engineers Paper 21877: Joint Rocky Mountain Section Meeting and Low-Permeability Reservoir Symposium, p. 705-716.

Lorenz, J. C., and Hill, R. E., 1992, Measurement and analysis of fractures in core, *in* Schmoker, J. W., Coalson, E. B., and Brown, C. A., eds., Geological studies relevant to Horizontal drilling: Examples from Western North America, Rocky Mountain Association of Geologists, p. 47-59.

Lorenz, J. C., Warpinski, N. R., and Teufel, L. W., 1996, Natural fracture characteristics and effects: The Leading Edge, v. 15, no. 8, p. 909-911.

Martinsen, O. J., Martinsen, R. S., and Steidtmann, J. R., 1993, Mesaverde Group (Upper Cretaceous), southeastern Wyoming: Allostratigraphy versus sequence stratigraphy in a tectonically active area: American Association of Petroleum Geologists Bulletin, v. 77, no. 8, p. 1351-1373.

McQuillan, H., 1973, Small-scale fracture density in Asmari Formation of southwest Iran and its relation to bed thickness and structural setting: American Association of Petroleum Geologists Bulletin, v. 57, no. 12, p. 2367-2385.

Merewether, E. A., 1990, Cretaceous formations in the southwestern part of the Powder River Basin, northeastern Wyoming: American Association of Petroleum Geologists Bulletin, v. 74, no. 8, p. 1337.

Muhlhaus, H. B., and Vardoulakis, I., 1988, The thickness of shear bands in granular materials: Geotechnique, v. 38, p. 271-284.

Murray, F. N., 1967, Jointing in sedimentary rocks along the Grand Hogback Monocline, Colorado: Journal of Geology, v. 75, no. 3, p. 340-350.

Murray, G. H., Jr., 1968, Quantitative fracture study - Sanish Pool, McKenzie County, North Dakota: American Association of Petroleum Geologists Bulletin, v. 52, no. 1, p. 57-65.

Narr, W., and Suppe, J., 1991, Joint spacing in sedimentary rocks: Journal of Structural Geology, v. 13, p. 1037-1048.

Nelson, R. A., 1985, Geologic analysis of naturally fractured reservoirs, Contributions in petroleum geology and engineering: Houston, Gulf Publishing Company, 360 p.

Nicol, A., Watterson, J., Walsh, J. J., and Childs, C., 1996, The shapes, major axis orientations and displacement patterns of fault surfaces: Journal of Structural Geology, v. 18, p. 235-248.

Oldow, J. S., Bally, A. W., Ave' Lallemant, H. G., and Leeman, W. P., 1989, Phanerozoic evolution of the North American Cordillera; United States and Canada, *in* Bally, A. W., and Palmer, A. R., eds., The geology of North America; an overview: Boulder, Geological Society of America, p. 139-232.

Olsen, D. K., Sarathi, P. S., and Hendricks, M. L., 1993, Case history of steam injection operations at Naval Petroleum Reserve No. 3, Teapot Dome Field, Wyoming: A shallow heterogeneous light-oil reservoir: SPE paper 25786, *in* International Thermal Operations Symposium, Bakersfield, CA, p. 93-110.

Pollard, D. D., and Aydin, A., 1988, Progress in understanding jointing over the past century: Geological Society of America Bulletin, v. 100, p. 1181-1204.

Potter, P. E., and Pettijohn, F. J., 1977, Paleocurrents and Basin Analysis: New York, Springer-Verlag, 425 p.

Price, N. J., 1966, Fault and joint development: Oxford, Pergamon Press, 176 p.

Prucha, J. J., Graham, J. A., and Nickelsen, R. P., 1965, Basement-controlled deformation in Wyoming Province of Rocky Mountains foreland: American Association of Petroleum Geologists Bulletin, v. 49, no. 7, p. 966-992.

Rice, D. D., 1983, Relation of natural gas composition to thermal maturity and source rock type in San Juan basin, northwestern New Mexico and southwestern Colorado: American Association of Petroleum Geologists Bulletin, v. 67, p. 1199-1218.

Roscoe, K. H., 1970, The influence of strains in soil mechanics: Geotechnique, v. 20, p. 129-170.

Sigda, J. M., Goodwin, L. B., Mozley, P. S., and Wilson, J. L., 1999, Permeability alteration in small-displacement faults in poorly consolidated sediments: Rio Grande Rift, central New Mexico, *in* Haneberg, W. C., Mozley, P. S., Moore, J. C., and Goodwin, L. B., eds., Faults and Subsurface Fluid Flow in the Shallow Crust AGU Monograph 113, p. 51-68.

Simon, J. L., Seron, F. J., and Casas, A. M., 1988, Stress deflection and fracture development in a multidirectional extension regime. Mathematical and experimental approach with field examples: Annales Tectonicae, v. 2, no. 1, p. 21-32.

Stearns, D. W., 1971, Mechanisms of drape folding in the Wyoming Province, *in* Renfro, A. R., Madison, L. W., Jarre, G. A., and Bradley, W. A., eds., Symposium on Wyoming tectonics and their economic significance, Wyoming Geological Association, p. 125-143.

Stearns, D. W., 1975, Laramide basement deformation in the Bighorn Basin - The controlling factor for structures in the layered rocks, *in* Exum, F. A., and George, G. R., eds., Geology and mineral resources of the Bighorn Basin, Wyoming Geological Association, p. 149-158.

Stearns, D. W., 1978, Faulting and forced folding in the Rocky Mountains foreland, *in* Matthews, V., III,, ed., Laramide folding associated with basement block faulting in the western United States, Geological Society of America, p. 1-37.

Stearns, D. W., and Friedman, M., 1972, Reservoirs in fractured rock, *in* King, R. E., ed., Stratigraphic oil and gas fields - classification, exploration methods, and case histories, American Association of Petroleum Geologists, p. 82-106.

Teufel, L. W., and Farrell, H. E., 1992, Interrelationship between in situ stress, natural fractures, and reservoir permeability anisotropy: A case study of the Ekofisk Field, North Sea, In Proceedings of Fractured and Jointed Rock Conference, Lake Tahoe, Ca, June 3-5, 1992, not consecutively numbered.

Thom, W. T., Jr., and Spieker, E. M., 1931, The significance of geologic conditions in Naval Petroleum Reserve No. 3, Wyoming, Professional Paper 163.

Tillman, R. W., and Martinsen, R. S., 1984, The Shannon self-ridge sandstone complex, Salt Creek Anticline area, Powder River Basin, Wyoming, *in* Tillman, R. W., and Seimers, C. T., eds., Siliclastic shelf sediments: Society of Economic Paleontology and Mineralogy Special Publication, p. 85-142.

Trexel, C. A., 1930, Compilation of data on Naval Petroleum Reserve No. 3 (Teapot Dome), Natrona County, Wyoming.

Unruh, J. R., and Twiss, R. J., 1998, Coseismic growth of basement-involved anticlines: The Northridge-Laramide connection: Geology, v. 26, no. 4, p. 335-338.

Wegemann, C. H., 1918, The Salt Creek oil field, Wyoming.

Weimer, R. J., 1960, Upper Cretaceous stratigraphy, Rocky Mountain area: American Association of Petroleum Geologists Bulletin, v. 44, no. 1, p. 1-20.

Weimer, R. J., 1984, Relation of unconformities, tectonics, and sea level changes, Cretaceous of Western Interior, U.S.A., *in* Schlee, J. S., ed., Interregional unconformities and hydrocarbon accumulation, American Association of Petroleum Geologists Memoir 36, p. 7-35.

Willis, J. J., and Brown, W. G., 1993, Structural interpretations of the Rocky Mountain Foreland: Past, Present, and Future, *in* Strook, B., and Andrew, S., eds., Jubilee Anniversary Field Conference Guidebook: Casper, Wyoming Geological Society, p. 95-119.

Wong, T.-f., 1998, Dilatancy, compaction and failure mode in porous rocks, *in* US Department of Energy Basic Sciences Geoscience Program, 1998 Research Symposium, Micromechanics and Flow, Santa Fe, NM, p. 14.

Wong, T.-f., David, C., and Zhu, W., 1997, The transition from brittle faulting to cataclastic flow in porous sandstones: Mechanical deformation: Journal of Geophysical Research, v. 102, no. B2, p. 3009-3025.

Distribution

Paul Basinski
El Paso Production
Four Greenway Plaza
Houston, TX 77046

Wallace Bayne
Bayne Geoscience
802 Tangigoot Drive
Aztec, NM 87410

Randal L. Billingsley
4 Wild Turkey Lane
Littleton, CO 80127
(303) 979-3559

Burlington Resources
PO Box 4289
Farmington, NM 87499-4289
Chip Head
Michael Dawson

Jock A. Campbell
Oklahoma Geological Survey
University of Oklahoma
Sarkeys Energy Center
100 E. Boyd Street, Room N-131
Norman, Oklahoma 73019-0628

Dan M. Cox
Veritas DGC Inc.
Exploration Services Division
10300 Town Park
Houston, TX77072

Murray Dahill
523 S. Park

Casper, WY 82601

New Mexico Institute of Mining and Technology
Department of Petroleum Engineering
Socorro, NM 87801
Larry Teufel
Tom Engler

Eric Erslev
Department of Earth Resources
College of Natural Resources
Colorado State University
Ft Collins, CO 80523

Mark P. Fischer
Department of Geology
Northern Illinois University
DeKalb, Illinois 60115-2854

Geospectrum, Inc.
214 W. Texas
Suite 1000
Midland, TX 79701
James J. Reeves
W. Hoxie Smith

Leo A. Giangiacomo
Extreme Petroleum Technology, Inc.
2033 Begonia St.
Casper, WY 82604

Catherine Hanks
Geophysical Institute
University of Alaska
Fairbanks, AK 99775

Hugo Harstad
Norsk Hydro
EPI-New Ventures
KJ 8.2
0246 Oslo, Norway

Bruce Hart
Earth and Planetary Sciences
McGill University
3450 University Street

Montreal, QC
CANADA H3A 2A7

Ralph L. Hawks, Jr.
Williams Energy
PO Box 3102
Tulsa, OK 74101

Peter H. Hennings
Geoscience Branch
Upstream Technology and Project Development
Phillips Petroleum Company
510 A Plaza Office Building
Bartlesville, OK 74004

Stephan A. Hines
Navajo Nation Oil and Gas Co. Inc.
P.O. Box 4439
Window Rock, AR 86515

James M. Hornbeck
Hornbeck Geological Consulting
5101 College Boulevard
Farmington, NM 87402-4709

Neil F. Hurley
Department of Geology and Geological Engineering
Colorado School of Mines
Golden, CO 80401

Robert Lemmon (10)
National Petroleum Technology Office
One West Third Street
Tulsa, OK 74103-3519

Alvis L. Lisenbee
Geology and Geological Engineering Department
South Dakota School of Mines and Technology
501 E. St. Joseph
Rapid City, SD 57701

Marathon Oil Co
100 West Missouri St
Midland, TX 79701
Jim Bucci
Jim Minelli

Tom Mather
Howell Petroleum Corp.
1111 Fannin St., suite 1500
Houston, TX 77002 – 6923

Curt McKinney
Devon Energy Corporation
20 North Broadway, Suite 1500
Oklahoma City, OK 73102-8260

Mark Milliken (20)
Rocky Mountain Oilfield Testing Center
907 N. Poplar
Suite 150
Casper, WY 82601

Jim Murphy
Conoco, Inc
600 North Dairy Ashford
Houston, TX 77079-1175

National Energy Technology Laboratories
PO Box 880
Morgantown, WV 26507-0880
Thomas Mroz (10)
James Ammer (5)
Gary Covatch
Mark McKoy

Ronald A. Nelson
BP Amoco
501 Westlake Park Blvd.
Houston, TX 77079-2696

New Mexico Institute of Mining and Technology
Department of Earth and Environmental Science
801 Leroy Place
Socorro, NM 87801
Laurel B. Goodwin (10)
Peter S. Mozley

New Mexico Bureau of Mines and Mineral Resources
New Mexico Institute of Mining and Technology

801 Leroy Place
Socorro, NM 87801-4796
Steven M. Cather
Ron Broadhead
Brian Brister

Joseph Piombino
BP Amoco Exploration
P.O. Box 3092
501 WestLake Park Boulevard
Houston, TX 77079-2696

Mr. Harry L. Siebert
14780 Highway 145
Dolores CO 81323-8200

John D. Taylor
River Gas Corporation
1300 McFarland Blvd. NE
Suite 300
Tscaloosa, AL 35406

Thomas L. Thompson
Thompson's Geo-Discovery, Inc.
580 Euclid Avenue
Boulder, Colorado 80302

Margot Timbel
Director, North American Exploration
ANSCHUTZ Exploration Corporation
555 Seventeenth Street
Suite 2400
Denver, CO 80202

US Geological Survey
Denver, CO 80225
Curt Huffman, MS 939
Steve Condon, MS 939

Jerry Walker
Independent Geologist
1455 Shewmaker Court
Reno, NV 89509

Yates Petroleum Corporation
105 South Fourth Street
Artesia, NM 88210
William R. Stanton
David B. Codding

Sandia National Laboratories
Albuquerque, NM 87185
Stephen Bauer, MS 0706
William Olsson, MS 0751
Marianne Walck, MS 0750
Scott Cooper, MS 0750 (20)
John Lorenz, MS 0750 (20)

Central Technical Files, 8945-1, MS 9018
Technical Library, 9616, MS 0899 (2)
Review and Approval Desk, 9612, MS 0612
For DOE/OSTI